Current Genetics (2019) 65:995–1014
https://doi.org/10.1007/s00294-019-00954-2

ORIGINAL ARTICLE

Impaired *GCR1* transcription resulted in defective inositol levels, vacuolar structure and autophagy in *Saccharomyces cerevisiae*

Chidambaram Ravi[1] · Ramachandran Gowsalya[1] · Vasanthi Nachiappan[1]

Received: 27 November 2018 / Revised: 1 March 2019 / Accepted: 8 March 2019 / Published online: 16 March 2019

Abstract

In yeast, the *GCR1* transcription factor is involved in the regulation of glycolysis and its deletion exhibited growth defect, reduced inositol and phosphatidylinositol (PI) levels compared to WT cells. We observed a down regulation of the *INO1* and *PIS1* expression in *gcr1*Δ cells under both I− and I+ conditions and the over expression of *GCR1* in *gcr1*Δ cells restored the growth, retrieved the expression of *INO1*, and *PIS1* comparable to WT cells. In the gel shift assay, the Gcr1p binds to its consensus sequence CTTCC in *PIS1* promoter and regulates its expression but not in *INO1* transcription. The WT cells, under I− significantly reduced the expression of *GCR1* and *PIS1*, but increased the expression of *KCS1* and de-repressed *INO1*. The Kcs1p expression was reduced in *gcr1*Δ cells; this reduced *INO1* expression resulting in abnormal vacuolar structure and reduced autophagy in *Saccharomyces cerevisiae*.

Keywords Phosphatidylinositol · Inositol · *PIS1* · *KCS1* · Autophagy

Introduction

Yeast has been widely used as a model system to study molecular biology and proliferative response to nutrients. Glycolysis regulation 1 (*GCR1)* is a transcription factor that tightly controls the expression of glycolytic genes (Willis et al. 2003; Clifton and Fraenkel 1981; Tornow et al. 1993; Barbara et al. 2006; Baker 1986) and serves as a regulator of RNA polymerase II transcription, while being involved in the coordinated regulation of cell cycle progression (Baker 1991; Willis et al. 2003). The Pho85 (cyclin-dependent kinase, CDK) is also involved in cell cycle regulation, responds to nutrient levels and is involved in *GCR1* regulation (Lenburg and O'Shea 2001). The loss of *PHO85* changes in many cellular events including the repression of *INO1* transcription, leading to inositol auxotrophy (Kliewe et al. 2017), and also affects *GCR1* transcription (Turkel et al. 2003). The deletion of *GCR1* does not affect the glucose 6-phosphate level, but accumulates trehalose and glycogen (Hossain et al. 2016; Seker and Hamamci 2003). The glycolytic intermediates dihydroxyacetone 1-phosphate (DHAP) and glyceraldehyde 3-phosphate (G3P) inhibit inositol 3-phosphate synthase activity in yeast and human (Shi et al. 2005). The inositol 3-P synthase (*INO1)*, is a rate-limiting enzyme that converts glucose 6-P to inositol 3-P which is further dephosphorylated to inositol by inositol monophosphatase (*INM1*) (Carman and Han 2011; Murray and Greenberg 2000). The glucose 6-phosphate from glycolysis is involved in the de novo synthesis of inositol, but the role of *GCR1* in inositol production is still uncertain.

In *Saccharomyces cerevisiae*, the inositol related molecules modulate diverse cell functions, such as phospholipid metabolism, anchoring of proteins in glycolipids (Carman and Han 2011), cell growth, membrane trafficking (Henry et al. 2012), and apoptosis (York et al. 2001). During inositol limitation (inositol auxotrophy) the Ino1p is highly expressed (Dubois et al. 2002), but the exogenous supplementation of inositol represses the *INO1* mRNA expression through the Opi1p (repressor protein). When the phosphatidic acid (PA) level drops, Opi1 is translocated from the ER to nucleus that interacts with Ino2p–Ino4p complex (Murray

Communicated by M. Kupiec.

Electronic supplementary material The online version of this article (https://doi.org/10.1007/s00294-019-00954-2) contains supplementary material, which is available to authorized users.

✉ Vasanthi Nachiappan
vasanthibch@gmail.com

[1] Department of Biochemistry, School of Life Sciences, Bharathidasan University, Tiruchirappalli, Tamil Nadu 620 024, India

and Greenberg 2000; Donahue and Henry 1981) and impairs the transcription of genes involved in phospholipid (PL) metabolism (Bachhawat et al. 1995). The phospholipids play an important role in cell size regulation, especially the increased PA levels modulate the cell size (Rao et al. 2017). Recent study shows that *INO1* promoter possesses a *cis*-acting Memory Requirement Sequence (MRS), which is essential for the binding of transcription factor Sfl1p, and *SFL1* (Heat shock factor-like DNA-binding domain) was reported to epigenetically control *INO1* transcriptional memory, and loss of Sfl1p disrupted *INO1* memory under inositol deprivation (D'Urso and Brickner 2017). The increased level of inositol up regulates the phosphatidylinositol synthase 1 (*PIS1*), and increases the PI levels required for progression of the cell cycle in yeast (Gardocki et al. 2005; Nikawa et al. 1987). The Zap1p transcription factor also controls *PIS1* expression under zinc depletion conditions through UAS_{ZRE} element in the promoter region (Carman and Han 2007; Han et al. 2005). Carbon source has an impact on *PIS1* expression (Anderson and Lopes 1996), and the *PIS1* promoter region contains a putative binding site for Gcr1p in UAS3 (Gardocki and Lopes 2003).

The inositol pyrophosphate synthase (Kcs1p) incorporates pyrophosphate to inositol hexakisphosphate (IP5) and inositol hexaphosphate (IP6) generating inositol pyrophosphates 5PP-IP4 and 5PP-IP5 (IP6 and IP7) in yeast, and regulates cellular processes like inositol metabolism (Ye et al. 2013), telomere length (Saiardi et al. 2005), vesicular trafficking (Saiardi et al. 2002), vacuolar biogenesis and stress response (Dubois et al. 2002). The phosphatidylinositol-3-kinase-related kinase (PIKK) is also the regulator of cell proliferation and genomic maintenance (Sugimoto 2018). The inositol pyrophosphate 5PP-IP4 (IP6) stabilizes the interaction of Ino2p–Ino4p complex and regulates *INO1* transcription (Ye et al. 2013). The 5PP-IP5 (IP7) transfers its pyrophosphate to the serine residues (S515–S518) of Gcr1p, thereby making Gcr1p unable to interact with Gcr2p, thus down regulating the transcription of the glycolytic enzymes (Szijgyarto et al. 2011). The Gcr1p interacts with Gcr2p (*GCR1* co activator) and forms a Gcr1p-Gcr2p complex that regulates the transcription of the glycolytic enzymes, which binds to the CTTCC binding motif in UAS sequence of the target glycolytic genes and positively regulates their expression (Willis et al. 2003). The removal of a Gcr1p binding site from the promoter region of Fatty acid synthase (*FAS1* and *FAS2*) genes resulted in a dramatic reduction of *FAS1* and *FAS2*-LacZ expression (Chirala 1992).

The absence of *INO1* disturbs the vacuolar structure under inositol limitation (Deranieh et al. 2015). Similarly, anti-epileptic drug Valproate (VPA) inhibits inositol-3-P synthase, and reduces the inositol level (Deranieh et al. 2015). However, the VPA treatment displayed abnormal vacuolar arrangements, also reduced V-ATPase activity and proton pumping under inositol limitation (Deranieh et al. 2015). The vacuole is the counterpart of the mammalian lysosome in yeast, besides being the key cellular site of protein and organelle turnover, and is also involved in proteolysis during micro and macro autophagy process (Stauffer and Powers 2017; Bryant and Stevens 1998; Li and Kane 2009).

Autophagy is maintained at a basal level under normal cell growth conditions and is induced by starvation (Wang and Klionsky 2003). PKA and TOR are two nutrient-responsive signaling components which help to maintain cell growth and autophagy (Kamada et al. 2010). PKA and TOR signaling pathways are regulated by the Rap1-mediated gene response and is based on the nutritional prominence (Santangelo 2006). Indeed, loss of *GCR1* reduces transcriptional activation of Rap1, likewise the exposure of rapamycin display no alteration in rapamycin sensitivity or rapamycin-induced down regulation of ribosomal protein gene expression (Menon et al. 2005; Lieb et al. 2001). The earlier reports suggest that the loss of *KCS1* displayed abnormal vacuolar structure, membrane abnormalities (Saiardi et al. 2002), defective autophagy flux and reduced autophagosome formation (Taylor et al. 2012).

In the current study, we focused on the functional importance of *GCR1* under inositol limitation and autophagy in *Saccharomyces cerevisiae*. We performed the growth analysis and investigated the gene expression of inositol biosynthesis. The *gcr1*Δ cells showed reduced intra-cellular inositol levels and the cells became inositol growth defective, which was alleviated by over expression of *GCR1* in the *gcr1*Δ cells. We also show that the deletion of *GCR1* decreased Kcs1p expression and our results suggest that *GCR1* deletion has an impact on *INO1* expression, vacuolar structure and autophagy process through the regulation of Kcs1p.

Materials and methods

Chemicals and media

Yeast extract, peptone, bacteriological agar, yeast nitrogenous bases (YNB) were purchased from Difco (Becton Dickinson and Company, Franklin Lakes, NJ, USA). YNB without inositol, LB media were obtained from HiMedia (Bengaluru, India). Thin-layer silica gel coated aluminum plate 60F254 and solvents were obtained from Merck (Bengaluru, India). Restriction endonuclease and T4 DNA ligase were procured from Fermentas. Glucose (GO) assay kit, ONPG (*O*-nitrophenyl-β-D-galactopyranoside), PMSF, glass beads, appropriate amino acid mixtures (drop out), anti-His antibody (Cat No: H1029), ALP conjugated secondary antibody (Cat No: A3562) and immunoblot developing substrate NBT/BCIP were from Sigma–Aldrich (Bengaluru,

India). Anti-TAP antibody (Cat No: CAB1001), anti-GFP antibody (Cat No: A-11122), anti-PGK antibody (Cat No: PA5-28612), nitrocellulose membrane, FM4-64 dye, Phusion high-fidelity DNA polymerase, dNTPs mix, cDNA synthesis kit and Power SYBR Green PCR Master Mix were obtained from Invitrogen (Bengaluru, India). *Myo*-inositol assay kit was obtained from Megazyme (New Delhi, India).

Plasmids, strains and growth conditions

The plasmids and yeast deletion strains used in the study are listed in Table 1. The wild type (BY4741: *MATa his3Δ1 leu2Δ0 met15Δ0 ura3Δ0*) and *gcr1Δ, gcr2Δ, opi1Δ, ino2Δ, ume6Δ* strains were gifted by Prof. Ram Rajasekharan, Central Food Technological Research Institute (CFTRI), Mysore, India, and they obtained it from EUROSCARF. The yeast cells were grown at 30 °C in YPD medium (1% yeast extract, 2% peptone and 2% glucose) and SC (synthetic complete) medium containing 0.67% yeast nitrogenous base, supplemented with the amino acids and 2% glucose. Synthetic nitrogen starvation (SD-N) containing 0.17% yeast nitrogenous base without ammonium sulfate and amino acids and 2% glucose were used to induce autophagy. Cloned plasmids were transformed in *Saccharomyces cerevisiae* strains by lithium acetate method (Gietz and Schiestl 2007). The yeast transformants harboring the plasmids pYES2-NT/B, YEp357R, pRS316 and pRS315, pRS415 were cultured in SD-Ura and SD-Leu medium containing 2%, 0.2% glucose or 1.8% galactose as required. SC or SD (Synthetic defined) media containing 75 µM inositol was symbolized as I+, whereas media lacking inositol was denoted I−. The cells were pre-cultured until mid-log phase in SC or SD media. Then the cells were collected and washed with fresh inositol-free media and divided into two parts. One part was shifted to I + and another part to I− media at 30 °C for indicated time points.

Analysis of inositol auxotrophy (I−) phenotypes

Yeast cells were grown in SC and SD media lacking leucine (SD-Leu) at 30 °C up to mid-log phase. Cells were harvested, and cell density was adjusted to $A_{600} = 1.0$. The cells were serially diluted (1:10, 1:100, 1:1000 and 1:10000) and 3 µl of cells were spotted onto SC-D or SC-Leu agar plates, with or without inositol supplementation (75 µM) and incubated at 30 °C for 3 days. For the growth curve analysis, cell growth was monitored by measuring the cell density (OD at A_{600}) at frequent time intervals until 64 h.

Glucose assay

Wild type (WT), *gcr1Δ* and *opi1Δ* strains were grown in synthetic complete (SC), and inositol-free medium at 30 °C with constant shaking at 180 rpm for 12 h. At indicated time points, 1 ml samples were collected and centrifuged and the supernatants were collected to determine the extra-cellular

Table 1 Strains and plasmids used in this study

Strains and plasmids	Characteristics description	Source
WT	BY4741; Mat a; *his3Δ 1 ; leu2Δ 0; met15Δ 0; ura3Δ 0*	Prof. Ram Rajasekharan
gcr1Δ	BY4741; Mat a; *his3Δ 1; leu2Δ 0; met15Δ 0; ura3Δ 0; YPL075w:: kanMX4*	”
gcr2Δ	BY4741; Mat a; *his3Δ 1; leu2Δ 0; met15Δ 0; ura3Δ 0; YNL199c:: kanMX4*	”
ino2Δ	BY4741; Mat a; *his3Δ 1; leu2Δ 0; met15Δ 0; ura3Δ 0; YDR123c:: kanMX4*	”
opi1Δ	BY4741; Mat a; *his3Δ 1; leu2Δ 0; met15Δ 0; ura3Δ 0; YHL020c:: kanMX4*	”
ume6Δ	BY4741; Mat a; *his3Δ 1; leu2Δ 0; met15Δ 0; ura3Δ 0; YDR207c:: kanMX4*	”
DH5α	F-ϕ80dlacZΔM15Δ (lacZYA-argF)U169 deoR recA1 endA1 hsdR17 (rk-mk-) phoA supE44λ thi-1 gyrA96 relA1	”
BL21(DE3)pLysS	F^- *ompT hsdSB* ($r_B^- m_B^-$) *gal dcm* (DE3) pLysS	”
pYES2/NT B	Yeast expression vector with N-terminal His6 tag fusion	,,
YEp357	Yeast episomal vector with *LacZ* reporter gene	,,
PIS1-LacZ	P_{PIS1}-*LacZ* reporter gene containing PIS1 promoter into YEp357	This study
pJH330	Contains 543 bp upstream of the INO1 ORF and 132 codons of the INO1 ORF fused in frame to the lacZ reporter in YEp357R	Prof. John M. Lopes
pRS315-GCR1	GCR1 clone constructed with self-promoter 484 bp 5′UTR + 2367 bp gDNA with intron + TAP 561 bp of the 3′UTR cloned into pRS315	Prof. Tracy L. Johnson
pKCS1	pYES2/ NT B yeast expression vector containing KCS1 gene	Prof. Rashna Bhandari
pRS415GPD	CEN/ARS plasmid P_{TDH3},T_{CYC1},LEU2marker	Prof. Ji-Sook Hahn
pRS415GPD-GCR1	GCR1 ORF cloned between the XbaI and XhoI sites of pRS415GPD	,,
pRS316–ATG8–GFP	ATG8 gene cloned into pRS316–GFP	Prof. Ravi Manjithaya

glucose concentrations using the glucose assay kit (Sigma Glucose-GO Assay Kit) according to the manufacturer's instructions.

Intracellular inositol assay

The WT and deletion strains were grown in SC media and cells were harvested after 12 and 24 h by centrifugation (4 °C) and washed with ice-cold water and resuspended in ice-cold 1 M perchloric acid for deproteinization. The cells were lysed using acid-washed glass beads for 10 min at 30-s interval, alternating with 30-s incubation on ice and pH 7.0 was attained with 1 M KOH solution (ice-cold). The cell extracts were centrifuged at 9000 rpm for 10 min at 4 °C. The supernatant was collected, and intra-cellular inositol was measured using *myo*-inositol assay kit (K-INOSITOL, Megazyme) according to the manufacturer's instructions.

RNA isolation and qRT-PCR analysis

Total RNA was extracted using the RNeasy kit from Qiagen according to manufacturer's instructions. Complementary DNA (cDNA) was synthesized using the high-capacity cDNA reverse transcription kit with 1 × RT buffer, 1 × random primer, 4 mM dNTP mix, 50 U/ml reverse transcriptase and 2 µg of total RNA. The primers were designed with the Primer Express R Software 3.0 (Applied Biosystems), and the sequences are listed in Table 2. For qRT analysis, 1 µl of diluted cDNA (1:20) sample was amplified using Applied Biosystems machine Step One Plus™ Real-Time PCR machine with the Power SYBR Green PCR master mix (Applied Bio systems). Samples were evaluated by the $^{\Delta\Delta}$Ct method (Livak and Schmittgen 2001). The mRNA expression levels were analyzed in triplicates, and the results were analyzed using relative quantification, with actin (*ACT1*) as an endogenous control. Data are represented as relative mRNA expression.

Preparation of cell-free lysate

The cells were harvested and centrifuged at 5000 rpm for 5 min, washed and cell extract was prepared by lysing the cells with glass beads and lysis buffer containing 50 mM Tris/HCl (pH 8.0), 1 mM $MgCl_2$, 10% glycerol and 1 mM phenylmethylsulfonyl fluoride (PMSF). Cells were vortexed for 30 s. The cells were kept on ice for 1 min between vortexing for all the 30 cycles. Unbroken cells were removed by centrifugation at 10,000 rpm for 10 min at 4 °C. Total protein was quantified (Bradford 1976) using BSA as standard.

Immunoblot analysis

For Western blotting analysis, proteins (50 µg) from cell extract were separated with 8% or 10% SDS–PAGE and transferred at 120 V for 2 h to the nitrocellulose membrane. The membrane was then incubated with primary anti-TAP antibody to detect Gcr1p (1:2000), anti-His antibody to detect Kcs1p (1:3000), anti-GFP antibody to detect Atg8p (1:2500), anti-Ape1 antibody to detect Ape1p (1:5000) and anti-Pgk1 to identify Pgk1p (1:5000) for 2 h at room temperature, followed by the ALP-conjugated goat anti-rabbit IgG secondary antibody for 1 h. The membrane was washed with PBST (0.1% Tween-20) and PBS. Finally, the blots were developed in the dark using the BCIP/NBT substrate. The intensity of Gcr1p and Kcs1p were normalized to the

Table 2 Primers used in this study

No.	Gene	Forward primer	Reverse primer
1	*ACT1 qRT*	ACTTTCAACGTTCCAGCCTTCT	ACACCATCACCGGAATCCAA
2	*INO1 qRT*	CAAGTCGGGACAAACCAAGT	ATAGGATGCAATGGAGACCG
3	*INO2 qRT*	TCAACCAAGCATGGGTTTTG	AAAACTGTTCAATGGCATTCGA
4	*INO4 qRT*	AGCTAAGCATGAGGCAAAAA	CCCAAATTAACTCCTTCGGTACTA
5	*INM1 qRT*	GTATTTTGAAAGAAGTGGGC	AATTGTTCCCCTCACAGCCA
6	*PIS1 qRT*	TGGACATGGTTACCGACAGA	TCGCCCACACTTTTATGAGA
7	*GCR1 qRT*	TTCGCTCACCTCAGCAGTTT	CCCCGCCTTCGTATCCTTTT
8	*TPI1 qRT*	ACCAGTCTGGGCCATTGGTA	TGTCACCCAACTTGGAAGCC
9	*KCS1 qRT*	ACCAACCTTCCTTGTTGCCC	CGGTGCCGAGTTTGGAGA
10	*GCR1* Clone	ATAGGATCCATGGTATGTACCAGCACGAG	ATACTCGAGAGATGGTGTATTATGTCGCC
11	*INO1 Pro*	ATAGGATCCCTATGTATATAGCGGATGAGTGC	GCGAAGCTTGGAGCAATATTATCTTCTGTCAT
12	*PIS1 Pro*	GCGGGATCCGTCACTTTCATTCTCAATGA	GCGCTGCAGTGTTGAATTCGAACTCAT
13	*KCS1 Pro*	GCGGGATCCTTGTTATTCCAAGACAAATGAAT	GCGCTGCAGAGTCTTTTAGCTTTAGTTTTAT
14	*TPI1 Pro*	AAGGATGAGCCAAGAATAAGGG	TTTTAGTTTATGTATGTGTTTTTTGTAG

qRT quantitative real-time PCR, *Pro* promoter

Pgk1p expression levels, and relative intensity was calculated using ImageJ analysis software (Abramoff et al. 2004).

Cloning, expression and purification of the recombinant His-tagged Gcr1 protein

Yeast genomic DNA was prepared as described previously (Sambrook et al. 1989). *GCR1* gene and *PIS1* promoter was amplified from yeast genomic DNA using the primers listed in Table 1. The *GCR1* gene was cloned into the *E. coli* expression vector pET28a using BamHI and XhoI restriction sites. *PIS1* promoter was cloned into the YEp357 vector using the BamHI and PstI sites. Clones were confirmed by double digestion and DNA sequencing. *E. coli* BL21 (DE3) cells harboring the pET28a-*GCR1* and pET28a vector control plasmids were precultured in 5 ml of LB medium with 50 µg/ml of kanamycin and grown overnight at 37 °C. The precultured cells were inoculated into 200 ml of 2 × LB medium containing 50 µg/ml of kanamycin and grown at 30 °C to an OD 0.4–0.6. The cells were induced with 0.5 mM IPTG (isopropyl β-D-1 thiogalactopyranoside) for 3–4 h at 30 °C. Cells were harvested and the cell pellet was resuspended with lysis buffer (50 mM Tris–HCl, pH 8.0, 300 mM NaCl, 10 mM imidazole, 0.2% Triton-X-100, 10 mM β-mercaptoethanol, 1 mM phenylmethylsulfonyl fluoride (PMSF), and 10% glycerol). The cells were lysed by sonication, and the lysed protein samples were centrifuged. The supernatant containing the recombinant protein having a $(His)_6$ tag was purified using Ni–NTA matrix and allowed to bind to the Ni–NTA beads at 4 °C for 4 h. The protein was eluted with lysis buffer containing 20 mM imidazole followed by a second wash (40 mM and 250 mM) imidazole in lysis buffer. A portion of the collected protein fraction was separated using 10% SDS–PAGE and protein expression was confirmed by immunoblotting using monoclonal His tag antibody as primary antibody (1:5000 dilution), and anti-mouse IgG-alkaline phosphatase as secondary antibody (1:2500 dilution) and developed with BCIP®-NBT substrate. The purified protein was used for EMSA studies.

Electrophoretic mobility shift assay (EMSA)

To visualize in vitro DNA–protein interactions, EMSA was performed using full-length Gcr1p and the promoters of *PIS1, TPI1, KCS1*, and *INO1* genes (1 kb) that were amplified from WT genomic DNA using the primers listed in Table 2. The gel purified PCR products were used for the gel shift assay. The binding buffer consisted of 10% glycerol, 20 mM Tris, pH-8.0, 50 mM KCl, 5 mM $MgCl_2$, 100 mM $ZnSO_4$, 5 mM β-mercaptoethanol, 1 mM dithiothreitol (DTT) and 10 mM HEPES–NaOH, pH 7.9. Purified Gcr1p was mixed with DNA in the presence of binding buffer and incubated for 25 min at 25 °C. The DNA–protein complex was resolved on non-denaturing polyacrylamide gel 6% with 0.5 × Tris borate–EDTA (TBE) running buffer. The gels were stained with SYBR Green® nucleic acid staining dye (Molecular Probes) and the complex was visualized under UV light at 300 nm using Bio-Rad ChemiDoc™ XRS + Imager (Hellman and Fried 2007; Rajvanshi et al. 2017).

Lipid extraction and analysis

The WT and *gcr1*Δ cells were grown on SC medium up to mid-log phase at 30 °C. The cells were collected and washed with fresh I− media and divided into two parts. One part was shifted to I+ and another part to I− media containing 2% dextrose and allowed to grow for 4 h. The cells grown up to mid-log phase (0 h and 4 h) with I− and I+ were harvested, and lipids extracted (Bligh and Dyer 1959). Briefly, chloroform and methanol were added to the cell pellet in 2:1 (v/v) ratio and vortexed, and an equal volume of acidified water (2% phosphoric acid) was added and again vigorously vortexed. The lipid containing organic layer was dried, and phospholipids separated by thin-layer chromatography on silica Gel TLC plates using chloroform/ methanol/ acetic acid (65:25:8; v/v) as the solvent system. The TLC plate was exposed to iodine vapor to visualize the lipids, scraped from the TLC plate and quantified (Rouser et al. 1966).

INO1-LacZ promoter reporter assay

The YEp357R-*INO1* and YEp357-*PIS1* plasmid containing transformants were selected and grown in SD-Ura medium containing 2% glucose. The cells were collected and washed with fresh SD-Ura I− media and resuspended in fresh I− and I+ (SD-Ura) media and incubated at 30 °C for 4 h. Cell-free extract was prepared, and an equal concentration of protein extract was used to measure β-galactosidase activity (Rose and Botstein 1983). The specific activity was expressed as nmol. min^{-1} mg^{-1} protein.

Fluorescence microscope

The yeast vacuoles were stained with the lipophilic dye FM4-64 (Molecular Probes) according to the procedure reported earlier (Vida and Emr 1995) with slight modification. The cells were grown in SC medium containing 2% glucose (I− media containing either presence or absence of inositol) at 30 °C with constant shaking. The cells were pelleted and resuspended with 500 µl of fresh medium containing 20 µM FM4-64 for 30 min, followed by washing with fresh medium and incubating with fresh medium for 1 h. The images were acquired on Zeiss LSM 700 confocal laser scanning microscope equipped with a 100X/1.40 oil objective and an AxioCam MRM camera (Zeiss). The yeast Atg8–GFP transformants were grown in an appropriate

medium, and the cells were collected and stained with FM 4–64 dye for visualizing the vacuolar membrane. The cells were viewed with an excitation wavelength of 488 nm for GFP and 515 nm for FM 4–64.

Statistical analysis

Experimental quantitative data were analyzed using Student's *t* test, and the differences were considered statistically significant when $*p < 0.05$ and $**p < 0.01$. Each experiment was repeated at least three independent repeats. Data are presented as the average ± standard deviation (SD). Statistical analysis was performed using the Sigma plot 10.0 software.

Results

Inositol depletion in *gcr1Δ* cells depicted growth defect

The role of *GCR1* in the synthesis of inositol, and growth was studied. Our results revealed that the growth of *gcr1*Δ cells was significantly reduced during inositol depletion (I− phenotype) condition when compared to the WT I−. Inositol limitation in the WT cells decreased the growth compared to inositol presence (Fig. 1a). However, the *gcr1*Δ cells under 75 μM inositol supplementation (I+) partially restored the growth defect (Fig. 1a). Further, the growth was studied using plate assay, which depicted growth defect under I − in *gcr1*Δ cells (Fig. 1b) and the supplementation of choline (100 mM) did not restore the growth and displayed strong inositol growth defect (Fig. S1a). The *opi1*Δ strain aids inositol overproduction (Fig. 1a, b) and serves as a positive control for inositol auxotrophy (Opi − phenotype) (Greenberg et al. 1982; Ye et al. 2013). Also, we tested diploid strain BY4743 and GCR1/*gcr1*Δ cell growth in the presence or absence of inositol and choline. The diploid strain, GCR1/*gcr1*Δ also exhibited a slight growth reduction on the I− C− and I− C + medium compared to wild type (BY4743) cells (Fig. S2). The GCR1/*gcr1*Δ displayed a semi-dominant growth defect under inositol limitation. However, the growth pattern of *gcr2*Δ was equivalent to WT (Fig. S1b and c). These results suggest that *GCR1* mutant exhibited growth defect under inositol deprivation.

GCR1 mutant reduced *INO1* expression and decreased intracellular inositol level

The glycolytic genes are regulated by *GCR1 t*ranscription factor (Willis et al. 2003), and glucose is essential for inositol production in yeast (Fig. 2a), and the perturbation of glycolysis affects the de novo inositol biosynthesis (Shi et al. 2005). The extracellular glucose and intracellular inositol levels were measured in WT, *gcr1*Δ and *opi1*Δ cells. We found that the rate of glucose utilization was reduced in *gcr1Δ* cells (Fig. 2b) and the intracellular inositol level was also reduced both at 12 (50%) and 24 h (59%) when compared with WT cells (Fig. 2d). The WT and deletion strains were grown up to mid-log phase and shifted to fresh I− media and the glucose measured at indicated time points. We found a rapid consumption of glucose in WT and *opi1Δ* cells when compared to *gcr1Δ* cells (Fig. 2c). The consumption of extracellular glucose was increased in the *opi1Δ* strain, and the intracellular inositol level was higher (Fig. 2b, d). A previous study suggested that the *INO1* expression was de-repressed under inositol limitation condition and it is via the Ino2–Ino4 transcriptional activation (Henry et al. 2012). In our study, the absence of inositol (I−) substantially up regulated the *INO1* (8.02-fold) and *INM1* (4.45-fold) expression in the WT cells (Fig. 2d). However, the *gcr1Δ* cells exhibited a significant down regulation of *INM1* (Fig. 2d), and *INO1* transcription both in the absence and presence of inositol compared to the WT. The *INO2* mRNA expression was also remarkably decreased in the *gcr1Δ* cells (Fig. 2e) and was independent of inositol level when compared to the WT cells. We simultaneously performed the *in vivo INO1* promoter activity in the *gcr1Δ* cells using the *INO1* promoter fused *LacZ* reporter assay. We observed a substantial reduction of β-galactosidase activity in the *gcr1Δ* cells during inositol absence (98.6 ± 6.8 nmol min^{-1} mg^{-1}), and presence (70.8 ± 4.3 nmol min^{-1} mg^{-1}) when compared to the WT cells (Fig. 2f). The meiotic transcriptional regulator *UME6* positively regulates the *CHO1, CHO2*, and *OPI3* but negatively regulates *INO1* as well as the phospholipid biosynthetic genes in yeast (Jackson and Lopes 1996). The *INO1* expression was observed both in repressing and derepressing conditions with *ume6Δ* cells (Jackson and Lopes 1996) and we also observed a substantial increase of β-galactosidase activity in the *ume6Δ* cells in both I–/I+ conditions. The *ino2Δ* strain was used as a negative control, whereas *opi1Δ* and *ume6Δ* mutant strains served as positive controls for *INO1-LacZ* reporter assay (Fig. 2f). Together, these results suggested that the growth defect in *gcr1*Δ cells could be accounted for the decrease in intracellular inositol and *INO1* mRNA expression.

Lack of *GCR1* depleted the cellular PI levels

The *INO1* expression was down regulated as well as the intra-cellular inositol level decreased in the *gcr1*Δ cells when compared to the WT cells. Further, we checked the effect of *GCR1* deletion on phosphatidylinositol (PI) levels. There was a significant reduction in the PI content (~ 33%) in *gcr1*Δ cells when compared to the WT cells in SC media (Fig. 3a). The WT and *gcr1*Δ cells were grown on SC media up to a mid-log phase and equal volume of culture was shifted to I− and

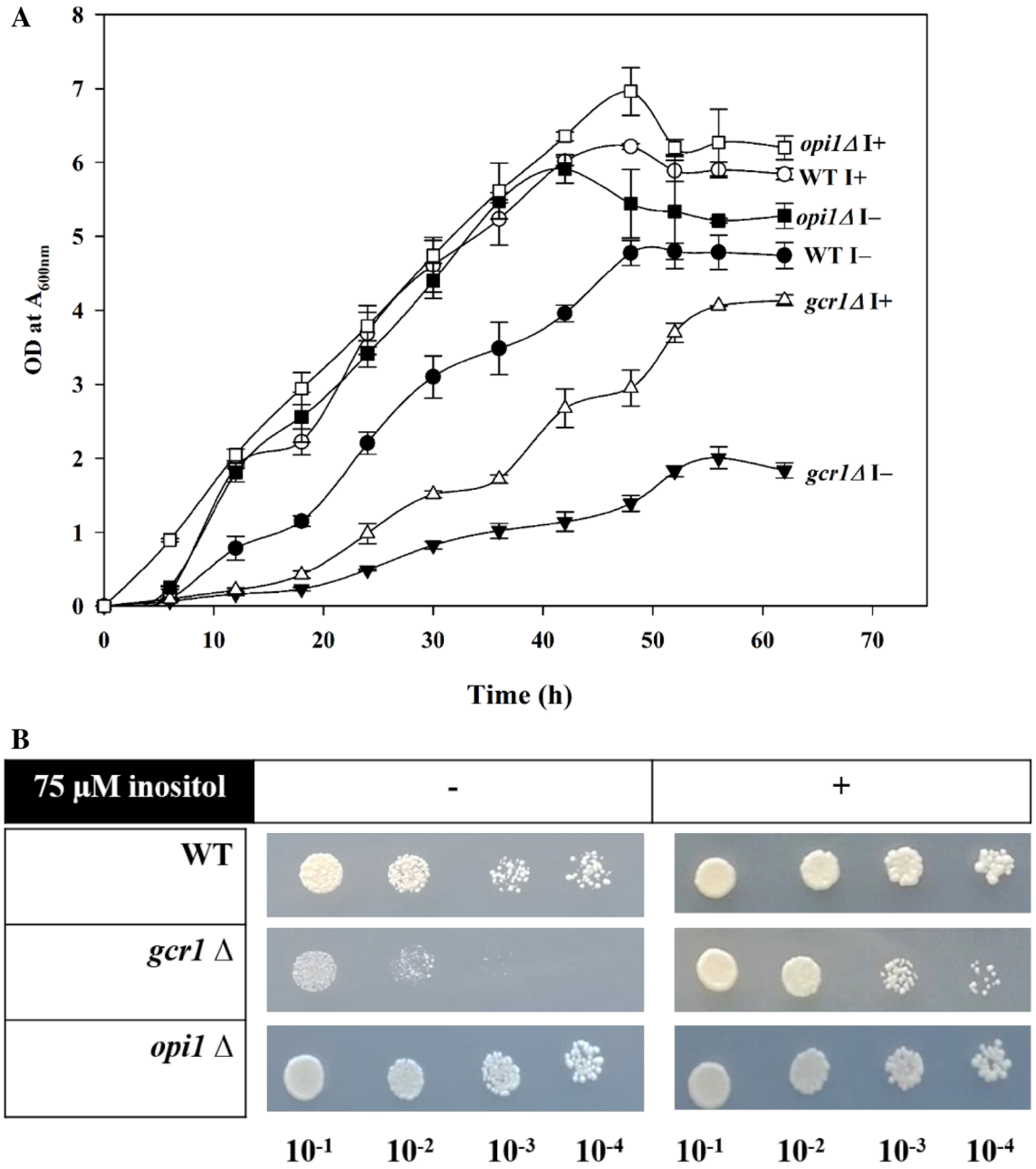

Fig. 1 Effect of inositol dependent growth in *gcr1Δ* cells. The WT, *gcr1*Δ and *opi1*Δ cells were grown in YPD medium up to mid-log phase at 30 °C. **a** Growth curve analysis. The cells were grown in the absence (I−) or presence (I+) of inositol. The growth curve was studied by measuring the OD ($A_{600\,nm}$) of the cells at indicated time points until 64 h. The growth curve is an average of three experimental repeats. **b** Spot test. The cells were normalized and equal number was serially diluted (tenfold dilution), and 3 µl of cells were spotted onto SC-D (SC-2% dextrose) agar plates, with or without inositol supplementation (75 µM) and incubated at 30 °C for 3 days

I+medium. After 4 h shift to the I+medium, we found an increased PI level in the WT cells relative to WT I− (Fig. 3a). Earlier study also suggested that the exogenous supplementation of inositol increases the rate of PI synthesis, and this could be due to the channelling of PA through CDP-DAG for PI synthesis, which led to a drop in the PA level (Loewen et al. 2004). The increase in PI content also depends on the fatty acids which are obtained from various sources including de novo fatty acid synthesis, TAG hydrolysis and PC turnover (Gardocki et al. 2005; Nikawa et al. 1987; Gaspar et al. 2006, 2011). Likewise, the inositol deprivation reduced the PI level in WT cells (Fig. 3a), and this reduction was accompanied with the accumulation of PA and CDP-DAG (Becker and lester 1977; Gaspar et al. 2006). The *gcr1*Δ cells showed a decrease

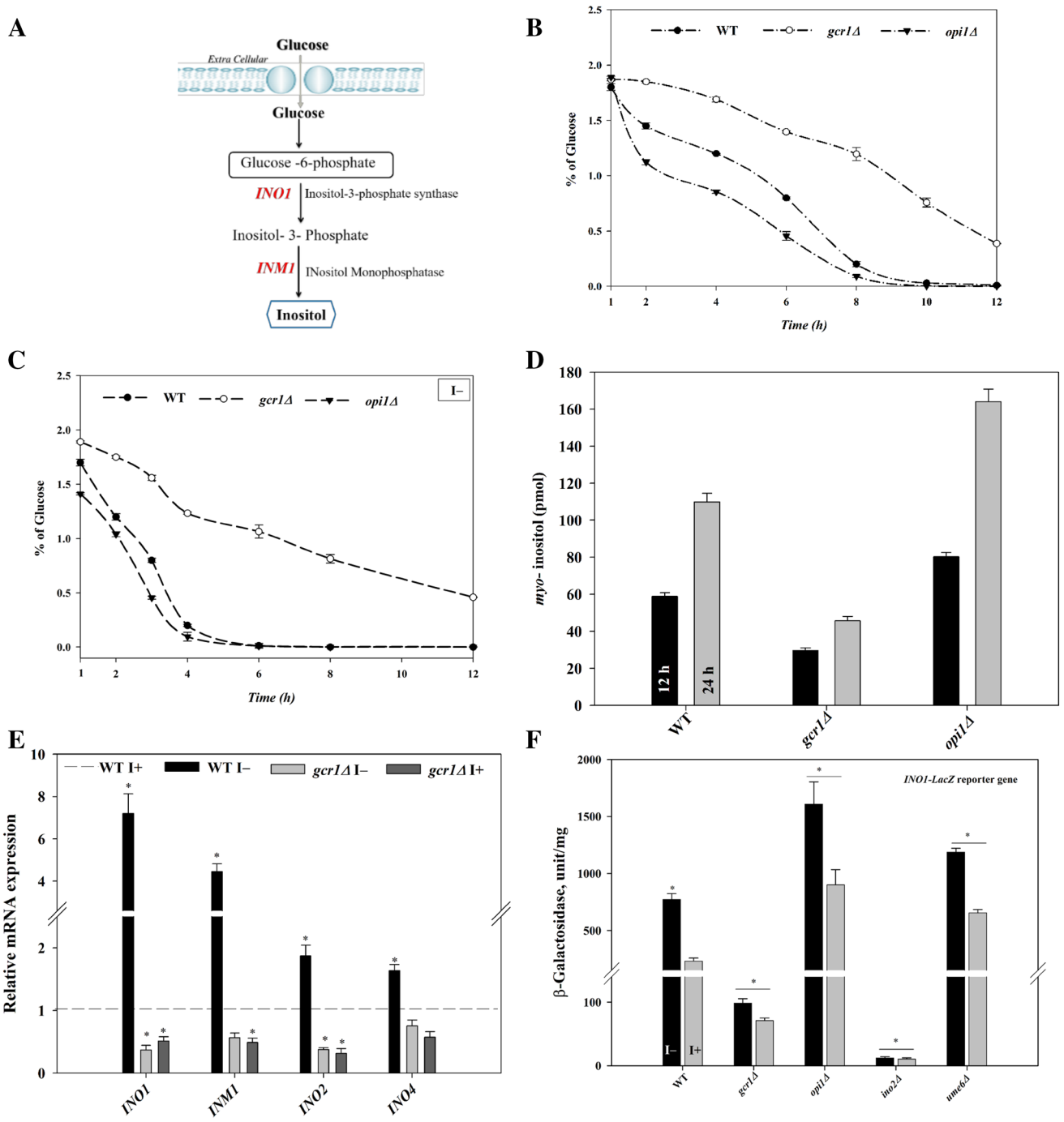

Fig. 2 Lack of *GCR1* depletes inositol production and down regulates *INO1* transcription. **a** The schematic diagram represents the inositol formation from glucose. **b** Analysis of glucose consumption. The WT, *gcr1*Δ and *opi1*Δ cells were grown in SC-D (2% dextrose) medium at 30 °C, and the extra-cellular glucose level was measured at indicated time points. **c** The glucose uptake was measured at indicated time points in WT, *gcr1*Δ and *opi1*Δ under inositol deprivation condition. **d** Intra-cellular inositol quantification. The WT, *gcr1*Δ and *opi1*Δ cells were grown in SC-D media and cells were harvested at 12 h or 24 h, and intra-cellular inositol was quantified as described under "Material and methods". **e** qRT-PCR analysis of *INO1, INM1, INO2*, and *INO4* gene expression. *ACT1* serves as an endogenous control. **f** β-Galactosidase activity of *INO1-LacZ*. The WT, *gcr1*Δ, *opi1*Δ, *ume6*Δ and *ino2*Δ cells were transformed with the *INO1-LacZ* fusion gene. The β-Galactosidase activity was measured as described under "Material and methods". The specific β-Galactosidase activity was expressed as units mg^{-1} (nmol min^{-1} mg^{-1}). The data shown are the mean ± SD (*$p < 0.05$) from three independent experiments

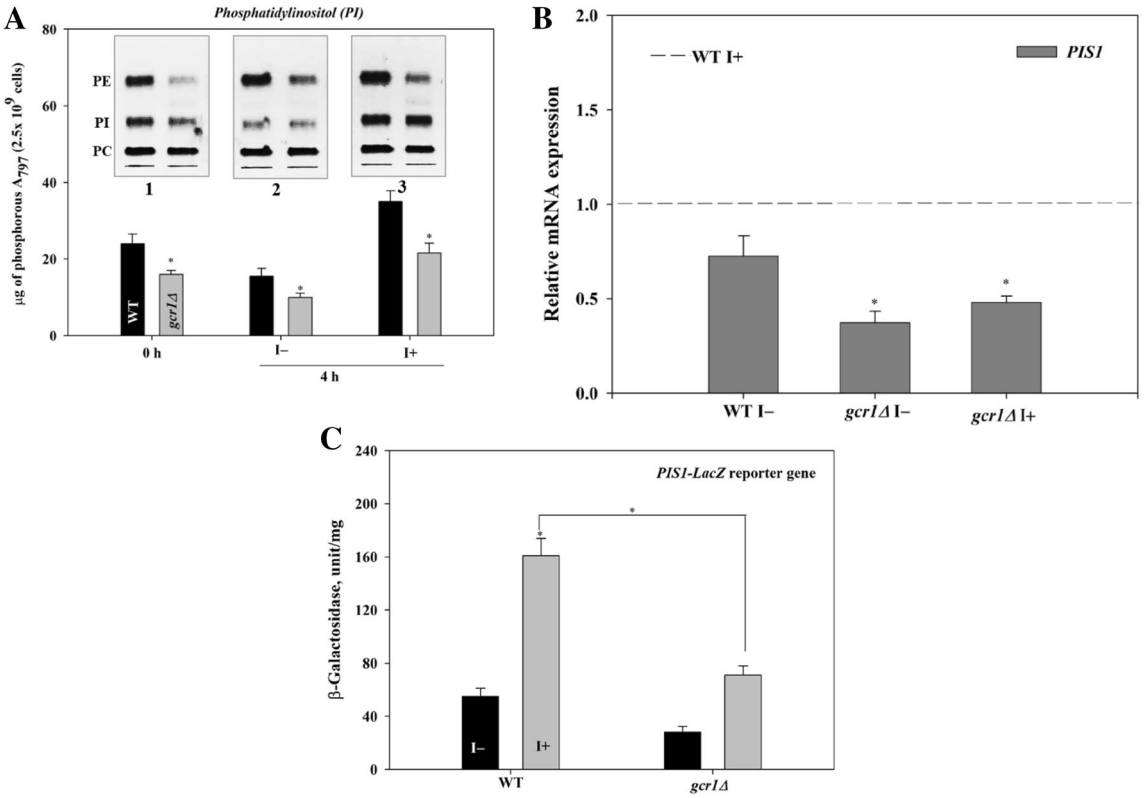

Fig. 3 Deletion of *gcr1*Δ alters the PI and down regulate *PIS1* expression. **a** Lipid analysis of WT and *gcr1*Δ cells. The cells were grown until mid-log phase in SC-D media at 30 °C, and cells were washed with I− media and resuspended with fresh I− and I+ media and grown up to 4 h. At this time point, cells were collected for lipid analysis ($A_{600\ nm}$ −100 OD) and resolved on silica TLC plate using solvent systems, chloroform/methanol/acetic acid (65:25:8, v/v). Phosphatidylcholine (PC); phosphatidylinositol (PI); phosphatidylethanolamine (PE). The PI was quantified as described in "Materials and methods". The inset represents iodine image of TLC plate. (1) Synthetic complete (SC); (2) I−; (3) I+ .The data shown are the mean ± SD (*$p < 0.05$) from three independent experiments. **b** Quantitative expression analysis of *PIS1* in the wild type and *gcr1*Δ in the presence or absence of inositol. *ACT1* was used as an endogenous control. The data shown is the average of three independent experiments (*$p < 0.05$). **c** β-Galactosidase activity of *PIS1-LacZ*. The WT, *gcr1*Δ cells were harboring YEp357 containing *PIS1-LacZ* fusion gene. The β-Galactosidase activity was measured as described under "Material and methods". The specific β-Galactosidase activity was expressed as units mg^{-1} (nmol min^{-1} mg^{-1}). The data shown are the mean ± SD (*$p < 0.05$) from three independent experiments

in the PI level both in I− (~33%) and I+ (~36%) compared to respective WT cells (Fig. 3a). The expression study of the *PIS1* gene in the *gcr1*Δ strain was down regulated both in the presence and absence of inositol compared to the WT I (Fig. 3b). The *PIS1* mRNA expression was confirmed by the promoter reporter activity using *PIS1-LacZ*. The β-galactosidase activity was substantially lowered in the *gcr1*Δ cells under I− and I+ compared to WT cells (Fig. 3c). These results suggested that the loss of *GCR1* significantly down regulated the *PIS1* expression and depleted the cellular PI level.

Inositol limitation altered the *GCR1* expression in WT cells

Further to confirm whether Gcr1 protein responds to inositol, we examined the effect of Gcr1p by shifting cells from SC to fresh I− and I+ medium. Over expression of *GCR1* in the WT cells (WT + pRS315-*GCR1*) decreased the expression of Gcr1p under I− condition when compared to I+ condition in the cells (Fig. 4a). Likewise, the presence of inositol up regulated (1.6-fold) and absence down regulated the mRNA expression of *GCR1* compared with WT cells at 0 h (Fig. 4b). The consensus sequence of Gcr1p binding motif is CTTCC (the CT box located in the upstream sequence of the genes (Baker 1991). It was reported that the *TPI1* possess two Gcr1p-binding sites (– 385 and − 345) in the UAS region, and Gcr1p is required for its transcriptional activation (Huie et al. 1992). Consistently Gcr1p regulating gene *TPI1* (triose phosphate isomerase 1) was up regulated (1.8-fold) under I + in WT cells. The transcription of *TPI1* and *GCR1* was set as '1' at '0' h and expression was decreased under I− condition when compared to I + in the WT cells (Fig. 4c). The Kcs1 protein expression was increased under I− condition (1.8-fold) when compared to

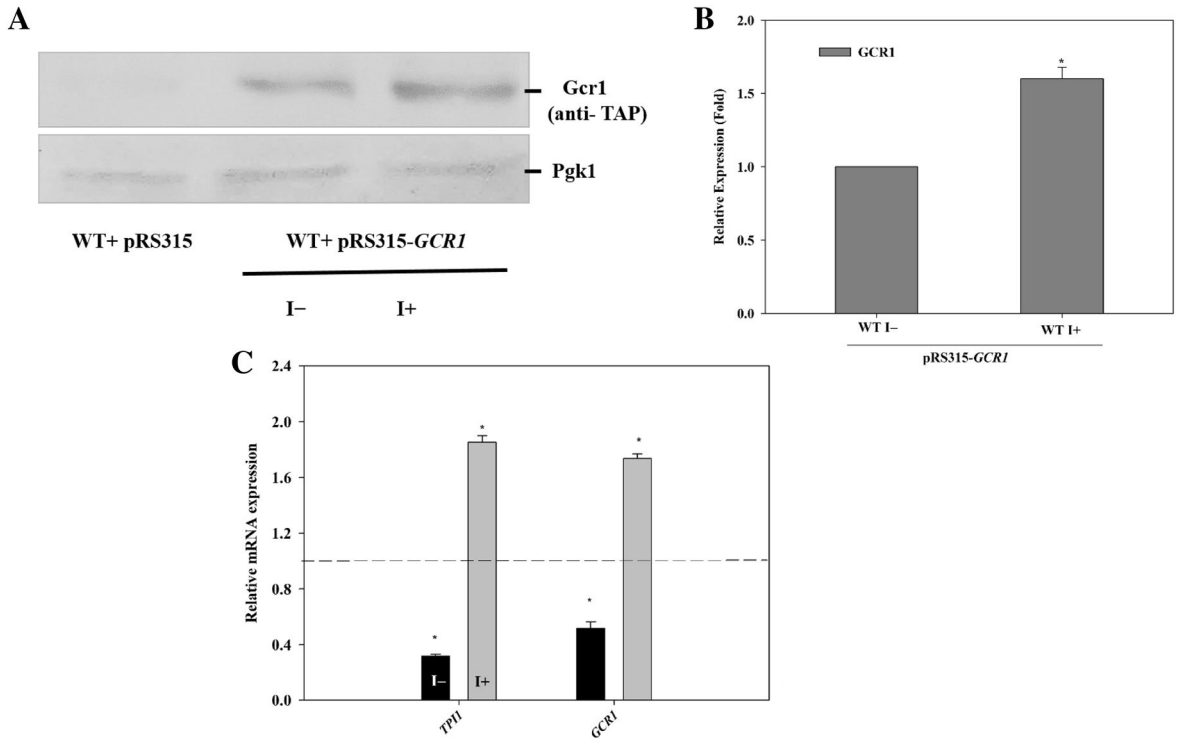

Fig. 4 Inositol limitation affects *GCR1* expression. **a, b** The protein expression of *GCR1* was measured using western blotting. The overnight culture of WT + pRS315 and WT + pRS315-*GCR1* strains were shifted to fresh SD-Leu media and grown up to 0.3 OD. The cells were washed with fresh SD-Leu I− medium and resuspended with I− and I + media, and after 4 h the cells were lysed and subjected to 8% SDS–PAGE. The western blot analysis was performed using anti-TAP tagged antibody to detect Gcr1 protein (109 kDa including TAP tag), and anti-Pgk1 (45 kDa) was the loading control. The Gcr1p expression was normalized by Pgk1p. **c** The qRT-PCR analysis measured the gene expression of *GCR1* and *TPI1*. The gene expression in wild type cells at 0 h was set as 1 (indicated horizontally as the dotted line) and the expression compared after 4 h both in the presence and absence of inositol. The data showed the mean ± SD of three independent experiments (*$p < 0.05$)

I + in the WT cells (Fig. 5c), but the *GCR1* expression was increased under I+ condition (Fig. 4a, b). It has already been reported that the *KCS1* expression negatively controls the Gcr1p mediated transcriptional regulation in yeast (Szijgyarto et al. 2011), and explains the decreased expression of Gcr1p under I− condition. The above result suggested that under inositol limitation the Kcs1p was increased and reduced Gcr1p expression.

GCR1 deletion decreased Kcs1p level

The Kcs1p (inositol pyrophosphate synthase) generates inositol pyrophosphate (5PP-IP4) that stabilizes the interaction of Ino2p–Ino4p complex regulating *INO1* transcription (Ye et al. 2013). The promoter reporter assay (*INO1*-LacZ) revealed a significant increase in the *INO1* activity under I− condition with the WT cells. The *INO1-LacZ* activity was significantly reduced in *kcs1*Δ under both (I− and I+) conditions (Fig. 5a) and similar results were observed in the *gcr1*Δ cells (Fig. 2d). We found a growth reduction in *gcr1*Δ cells during I− condition (Fig. 1) and the *kcs1*Δ cells also showed a similar pattern (Fig. 5a). The *kcs1*Δ cells affected cellular inositol production, down regulated *INO1* transcription and decreased PI level (Ye et al. 2013) and we observed similar results with *gcr1*Δ cells. Compared to the WT cells, significant down regulation of *KCS1* expression was observed in the *gcr1*Δ cells (Fig. 5b). The Kcs1p expression was significantly increased in the WT + pYES2-*KCS1* cells under I − condition and decreased under I + condition, whereas the Kcs1p expression was significantly decreased (both in the I− and I+) in the *gcr1*Δ+pYES2-*KCS1* cells, compared to WT I− cells (Fig. 5c). The *INO1* expression was down regulated in both I- and I + in *gcr1*Δ cells (Fig. 2d). Aforementioned, Kcs1p is important for inositol auxotrophic growth and *INO1* transcription (Ye et al. 2013). Thus, the reduced *INO1* expression in the *gcr1*Δ cells might be accounted for the decreased expression of Kcs1p (Fig. 5c).

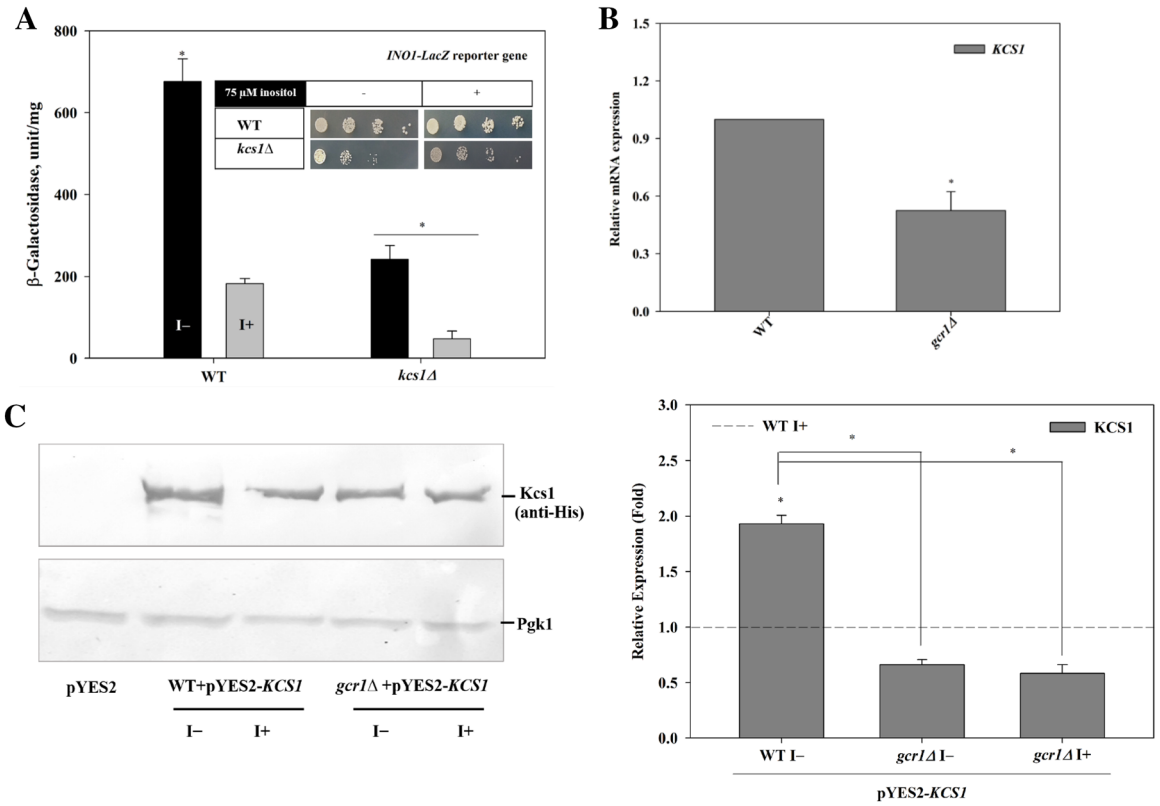

Fig. 5 Role of *KCS1* in *GCR1* deletion cells under inositol limitation. **a** Cell growth and *INO1- LacZ* promoter reporter activity under inositol presence and absence condition in WT and *kcs1*Δ cells. **b** The *KCS1* mRNA expression of WT and *gcr1*Δ cells grown with SC media. **c** The Kcs1p expression was measured using western blotting. The WT and *gcr1*Δ cells were over expressed with YES2-*KCS1* and grown in SD-Ura (0.2% dextrose and 1.8% galactose) medium up to mid-log phase, the cells were washed and resuspended with I− or I+ medium. After 4 h the cells were lysed and subjected to 8% SDS–PAGE and Western blot was analyzed using anti-His tag antibody (to detect Kcs1p of size 126 kDa including His tag), and anti-Pgk1 (45 kDa) was the loading control. Kcs1p expression was normalized by Pgk1p and the data showed the mean ± SD of three independent experiments (*$p < 0.05$)

Enzymatic mobility shift assay (EMSA) confirms the binding of Gcr1p to promote the expression of *PIS1*

Transcription factor Gcr1p activates the diverse set of genes involved in glycolysis, RNA polymerase II and cell cycle regulating genes (Willis et al. 2003; Barbara et al. 2006; Baker 1986). We examined the in vitro analysis of DNA–protein interactions, and for this the full-length *GCR1* was cloned into pET28a and expressed in BL21 pLys DE3 cells. The recombinant protein was purified using Ni^{2+} -NTA affinity chromatography and the purity confirmed by immunoblotting with anti-His tag monoclonal antibody (Fig. 6b). The in silico analysis we found Gcr1p binding site 5′CTTCC 3′ (CT Box) in the promoter region (upstream) of the *PIS1* (– 885, – 735, – 690 and – 537) and *INO1* (– 611, -596 and – 384) genes using YEASTRACT promoter database of *S. cerevisiae*. A previous study suggested that the Gcr1p positively regulates *TPI1* expression in yeast (Huie et al. 1992). The Gcr1p binding site (CTTCC) is present at two positions (– 385 and – 345) on the promoter of *TPI1* and serves as a positive control for EMSA. We performed an EMSA with 1000 bp region of the promoter of *TPI1, INO1, PIS1* and *KCS1* amplicon. The purified Gcr1p strongly binds with *TPI1* promoter, which possesses two CT box binding site in the UAS region (Fig. 6c). On the other hand, the Gcr1p did not form a binding complex of *INO1* promoter, even with the increasing concentration of Gcr1p (Fig. 6d). The *KCS1* promoter does not possess CT box binding site, and so no binding complex was formed (Fig. 6e). Surprisingly, with the 1000 bp from the promoter region of the *PIS1* and the purified Gcr1p, an increase in DNA–protein binding complex was observed with increasing concentration of Gcr1p (Fig. 6f). The above result suggested that the Gcr1p is an important for the activation of *PIS1* but not for *INO1* and *KCS1* transcription.

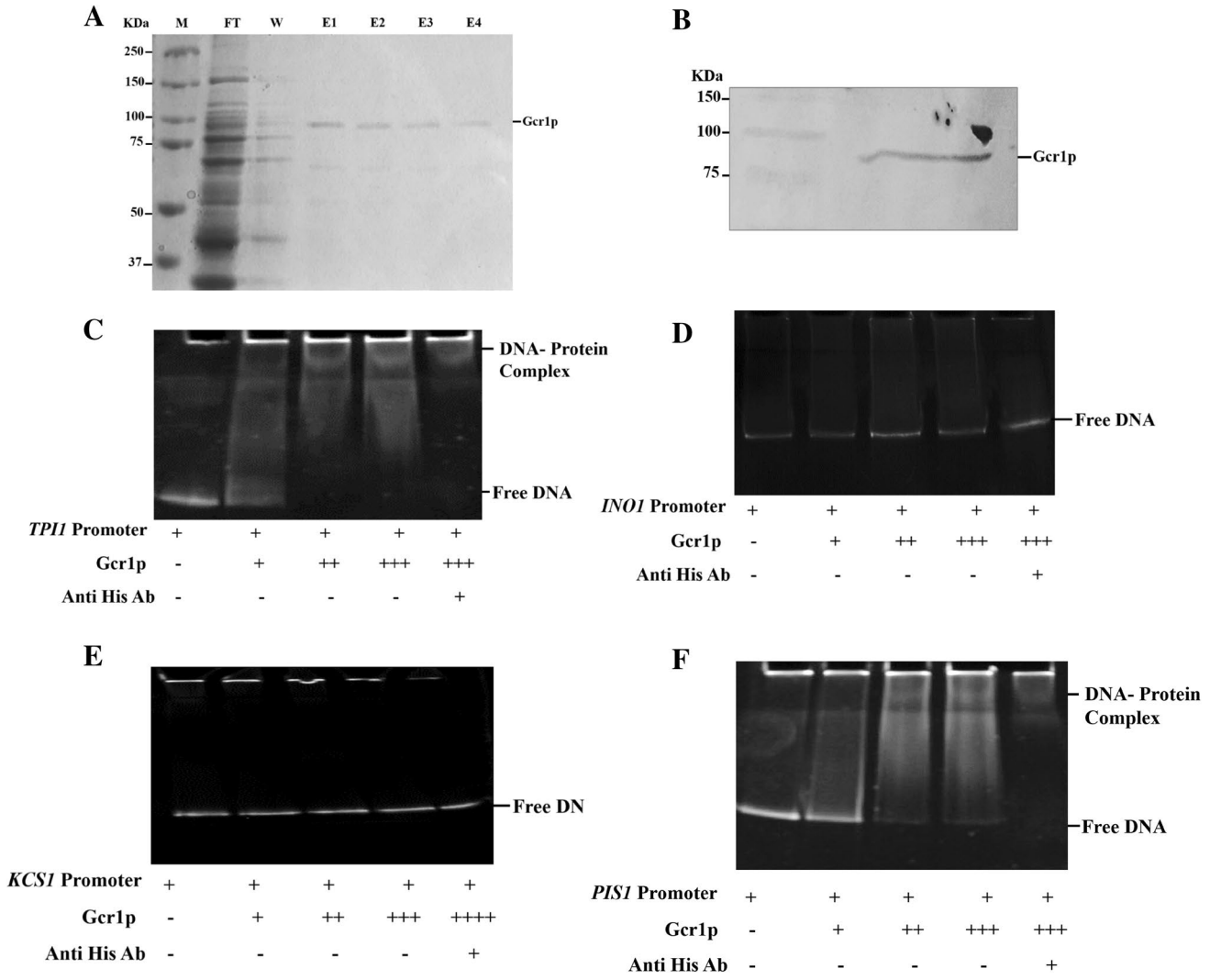

Fig. 6 Purification of Gcr1p and EMSA. **a** Purification of Gcr1p. The bacterially expressed recombinant Gcr1p was purified using nickel affinity chromatography and resolved on a 10% SDS–PAGE and stained with Coomassie brilliant blue (CBB Staining). *M* marker, *FT* flow through, *W* wash, E1–E4 eluted fractions of purified protein. **b** An immunoblot of Gcr1p using anti-His tag antibody. **c** EMSA of Gcr1p with *TPI1* promoter **d** EMSA of Gcr1p with *INO1* promoter **e** and **f** EMSA of Gcr1p with *KCS1* and *PIS1* promoters

GCR1 expression in *gcr1Δ* alleviates the inositol growth defect

The *gcr1*Δ strain depicts inositol dependent growth defect and we checked the impact of *GCR1* overexpression in *gcr1*Δ. The over expression of *GCR1* in the *gcr1*Δ cells (pRS415-*GCR1*) restored the growth as in WT cells (with both I− and I+) unlike the *gcr1*Δ +pRS415 cells (Fig. 7a). The β-galactosidase activity of *INO1* with the *gcr1*Δ+ pRS415-*GCR1* cells (in both I− and I + condition) reverted as seen with WT cells (Fig. 7b). Over expression of *GCR1* gene in WT cells increased *PIS1*-LacZ activity under exogenous supplementation of inositol (Fig. 7c), which indicates Gcr1p positively controls *PIS1*. The *INO1* expression in WT + pRS415-*GCR1* and WT + pRS415 (in I− or I + condition) were similar (Fig. 7b). The over expression of WT + pRS425-*GCR1* did not change *INO1* transcription under inositol deprivation condition (Fig. 7b). The IP7 formed by Kcs1p donates the pyrophosphate to the phosphorylation site of Gcr1p, inactivating the Gcr1p-Gcr2p complex formation, as a result disturbing the Gcr1 mediated regulation (Szijgyarto et al. 2011).

Lack of *GCR1* affects vacuolar morphology

The loss of Kcs1p displayed accumulation of small vacuolar structure and abnormal vacuolar membrane formation (Dubois et al. 2002). We examined the effect of *GCR1* on vacuolar morphology, using the lipophilic dye FM 4–64. We visualized the yeast vacuoles, in SC media and the WT cells

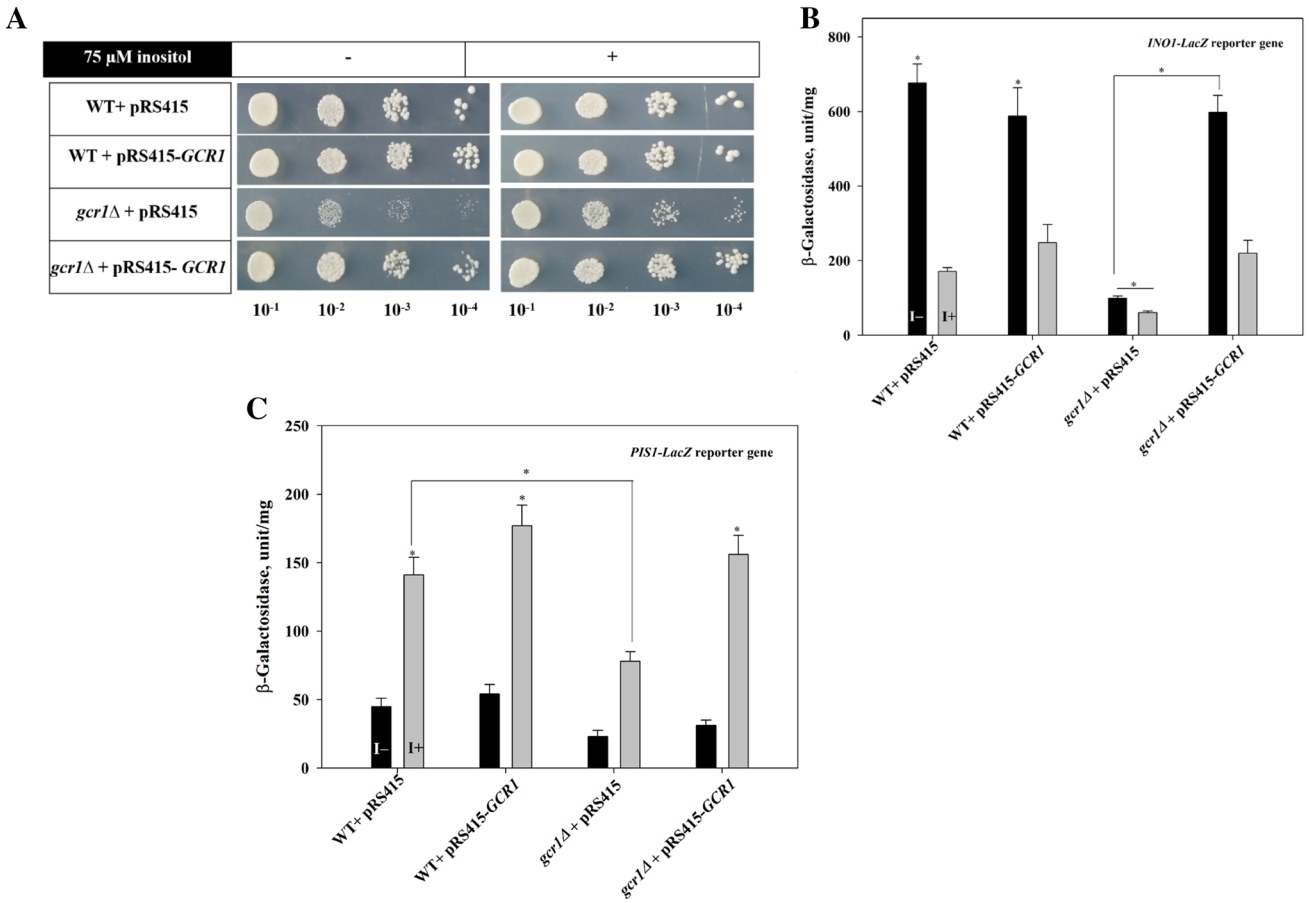

Fig. 7 Plate assay and promoter reporter assay under *GCR1* over expression. **a** The spot test analysis (agar plates of SD-Leu + 2% dextrose, incubated for 3 days at 30 °C) was performed in wild type and *gcr1*Δ cells, transformed with pRS415 or pRS415-*GCR1* under I− and I + condition. The data is a representative of the experiment repeated thrice. **b, c** The WT and *gcr1*Δ cells containing pRS415 and pRS415-*GCR1* cells were co-transformed with *INO1-LacZ* fusion gene or *PIS1-LacZ* fusion gene and cells were grown up to mid-log phase in SD-Leu-Ura media. The cells were washed with fresh SD-Leu-Ura I− and seeded into the same media, either in the presence or absence of inositol. After 4 h induction, the cells were extracted, and the *INO1*-promoter activity or *PIS1*-promoter activity was assayed by measuring the β-Galactosidase activity that was expressed in units mg^{-1} (nmol min^{-1} mg^{-1}). The assay represents the mean ± SD of three independent experiments (*$p < 0.05$)

contain 1–3 vacuoles per cell (Fig. 8a, b), and inositol presence did not effect on the vacuole number or morphology (Fig. S3a–d). Unlike the WT cells, the *gcr1*Δ cells showed a substantial increase in the fragmented vacuoles (46% of cells display ≥ 4 vacuoles per cell). Normally, Kcs1p deletion affected dynamic cellular process including vacuolar membrane abnormality (Dubois et al. 2002). We observed an increase in the vacuolar number (75% of cells displayed ≥ 4 vacuoles per cell; Fig. 8a, b) with *kcs1*Δ cells in SC media. The *INO1* expression is important for normal vacuolar morphology under inositol deprivation (Deranieh et al. 2015). We also observed an increase in the vacuolar fragmentation in *gcr1*Δ (67% of cells contain ≥ 4 vacuoles per cell Fig. S3a and b) cells under I − condition compared with WT I−. The addition of inositol altered the vacuolar morphology in the *gcr1*Δ (45% of cells contain ≥ 4 vacuoles) and *kcs1*Δ (58% of cells display ≥ 4 vacuoles per cell) cells when compared to WT I + cells (Fig S3c and d). Indeed, the *gcr1*Δ cells showed an alteration of vacuolar structure similar to *kcs1*Δ cells (Fig. 8a). The above result suggested that the lack of *GCR1* reduced Kcs1p, possibly affecting vacuolar membrane morphology.

Deletion of *GCR1* led to a defect in autophagy degradation

The vacuoles play an important role for cellular pH maintenance, response to osmotic shock, nutrient deprivation, and ion-homeostasis, specifically major site for intracellular proteolysis as well as micro and macroautophagy (Stauffer and Powers 2017; Li and Kane 2009). Normally, Atg8–GFP has been extensively used to observe the process of Cvt pathway and autophagy where Atg8–GFP is embedded in the inner membrane of the completed

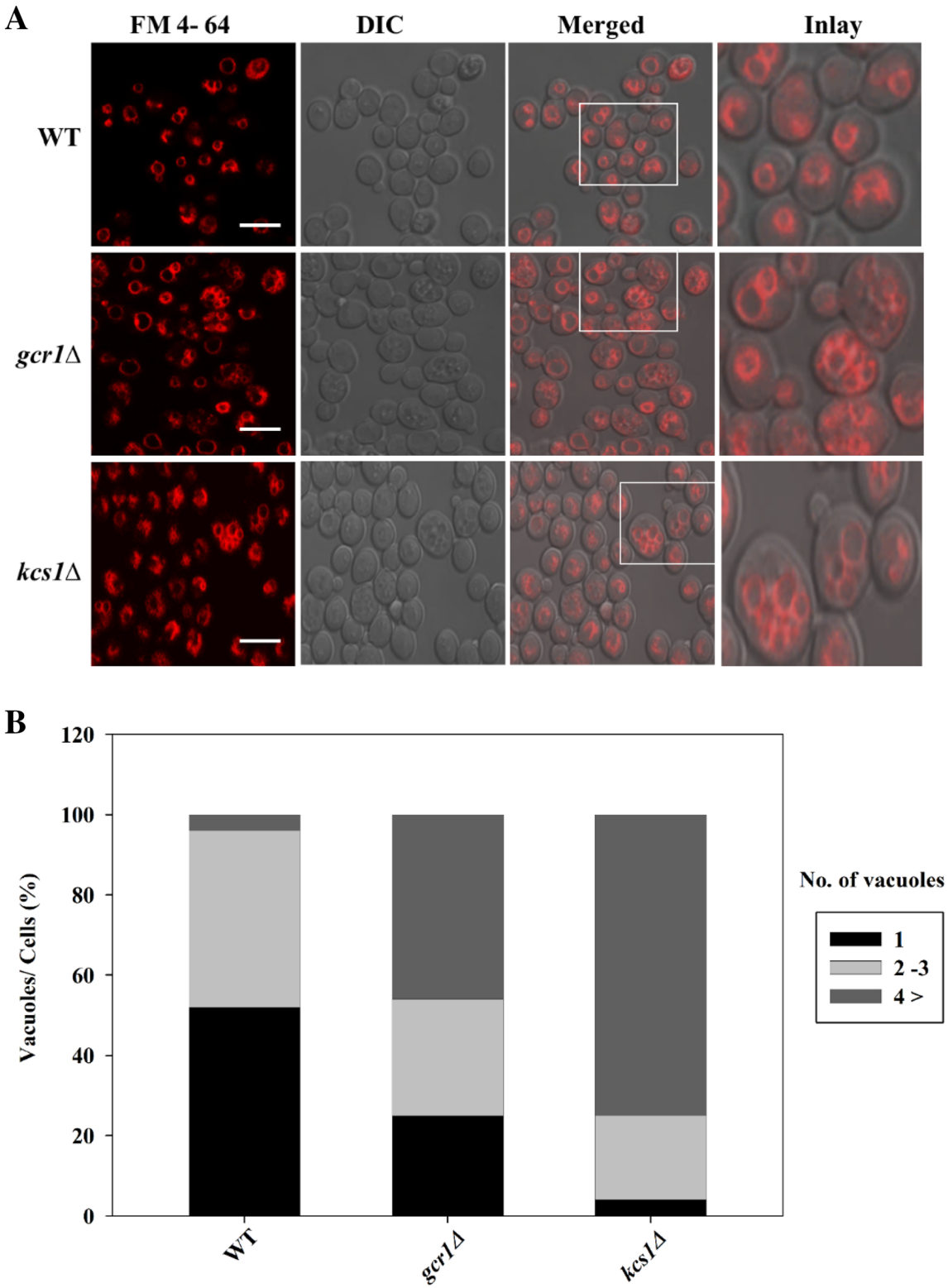

Fig. 8 Visualization of vacuolar morphology. The WT, *gcr1*Δ and *kcs1*Δ cells were grown in SC medium up to mid-log phase and equal volume of culture was collected and vacuoles stained with FM4-64 lipophilic fluorescent dye as described under "Materials and methods". **a** Vacuolar morphology of WT, *gcr1*Δ, and *kcs1*Δ cells. **b** Quantification of labeled vacuoles per cell ($n > 100$ cells per stain). Images were observed by laser scanning confocal fluorescence microscope (LSM710-Zeiss). Scale bar, 5 µm

autophagosome. The synthesis of Atg8 is very low under vegetative growth and is induced upon starvation (Suzuki and Ohsumi 2007) and the autophagic flux was monitored by Atg8–GFP processing (Shintani and Klionsky 2004). The *gcr1*Δ cells decreased Kcs1 expression, and as a result an increased the number of vacuoles (Figs. 5c and 8). The WT, *gcr1*Δ, *atg1*Δ and *kcs1*Δ cells were transformed with pRS316–ATG8–GFP plasmid and the transformants were grown to mid-log phase in SD-Ura with 2% dextrose (0 h), then the cells were pelleted and shifted in to SD-N media for 4 h or 8 h. The immunoblot analysis of Atg8–GFP was monitored using anti-GFP antibody. The WT cells generate free GFP under SD-N after 4 h, which indicates the translocation of Atg8–GFP to intravacuolar vesicles for Atg8–GFP degradation (Fig. 9a). However, the GFP molecule is more resistant to vacuolar protease, so the GFP accumulation is indicative of autophagic flux. Compared with the WT cells, the *gcr1*Δ cells had no free GFP under SD-N, similar to the *atg1*Δ and *kcs1*Δ cells (Fig. 9a). The autophagy defect was monitored by determining the delivery of Atg8–GFP to the vacuoles by fluorescence microscopy. The cells from mid-log phase, were shifted to SD-N media and grown for 4 and 8 h, and cells were collected and stained with FM 4–64 dye and examined under Axio Observed 3 Inverted fluorescence microscope (Zeiss). The WT cells, accumulated Atg8–GFP in the perivacuolar region known as phagophore assembly site (PAS) associated with FM 4–64 vacuolar membrane, while the autophagy deficient *atg1*Δ failed to accrue PAS and was dispersed in the cytoplasm. The *gcr1*Δ cells develop single PAS under mid-log phase (Fig. 9b). The WT cells accumulate GFP signal inside the vacuoles under SD-N at 4 and 8 h, indicating the efficient occurrence of autophagy flux (Figs. 9b and S3a). As a negative control, *atg1*Δ failed to accumulate GFP inside the vacuolar membrane. Similarly, reduced vacuolar GFP accumulation was found *gcr1*Δ cells both at 4 and 8 h under SD-N grew cells, indicating reduced autophagy than the WT cells (Figs. 9b and S3a). Compared to the WT cells, the co-localization percentage reduced in *gcr1*Δ (15% and 22% in SD-N 4 and 8 h) cells (Fig. S3b). Similarly, the *gcr1*Δ cells increased Atg8–GFP punctuate in cytosol under nitrogen starvation condition (Fig. 7c and Fig. S3a and c). Additionally, we also analyzed the function of the Cvt pathway using an anti-Ape1 antibody to detect cytoplasmic protein aminopeptidase 1 (Ape1) expression. Immunoblotting results show that the *gcr1*Δ cells under nitrogen starvation have a defect in mature Ape1 formation (Fig. 9d). In the *atg1*Δ (autophagy mutant) cells the mature Ape was not observed in both vegetative and starvation conditions (Fig. 9d). The results strongly suggest that the lack of *GCR1* affects autophagosome biogenesis contributing to the deficiency in autophagy flux.

Discussion

The Gcr1p is a known transcription factor that regulates glycolysis, ribosomal protein, cell cycle and RNA polymerase II in growing yeast cells (Willis et al. 2003; Clifton and Fraenkel 1981; Tornow et al. 1993; Barbara et al. 2006; Baker 1986). In the present study, we demonstrated that *gcr1*Δ cells affect inositol production, and cells displayed inositol dependent growth defect. Here we also report that the deletion of *GCR1* displays abnormal vacuolar structure and defective autophagy flux.

The transcription factor *GCR1* positively regulates the transcription of glycolytic genes (Baker 1986). The mutant *TPI1* exhibited a growth defect under inositol limitation, leading to an increase in DHAP (Dihydroxyacetone phosphate) production that inhibited the inositol-P synthase activity (Shi et al. 2005). On the contrary, in *gcr1*Δ strain the glycolytic intermediate product DHAP was reduced (Willis et al. 2003), and growth defect was observed under I− condition. The growth curve and plate assay revealed that the cells lacking Gcr1p reduced the growth under inositol deprivation (Fig. 1), and the growth was partially restored upon inositol supplementation compared to the WT cells (Fig. 1). However, choline supplementation was not able to restore the growth (Fig. S1). As shown in Fig. 2, deletion of *GCR1* delayed glucose consumption and reduced intra-cellular inositol level when compared with the WT cells. The WT and *opi1*Δ strains rapidly consumed the glucose under I− condition (Fig. 2c). This could be due to the activation of de novo inositol biosynthesis, under inositol limitation. The glucose-6 P is the substrate for inositol-3 P synthase that forms inositol-3 P, and is consequently dephosphorylated to form inositol. The *INO1* (inositol-3 P synthase) is the hallmark gene for inositol auxotrophy (Henry et al. 2012; Ye et al. 2013; Shetty and Lopes 2010). In response to inositol depletion, *gcr1*Δ cells displayed down regulation of *INO1* mRNA expression (Fig. 2e) and reduced β-galactosidase reporter (for *INO1-LacZ* activity) assay compared to WT cells (Fig. 2f) and is associated with inositol dependent growth defect. We conclude that the inositol defect in *gcr1*Δ cells is caused by defective *INO1* transcription. In *Saccharomyces cerevisiae*, the Ino2p and Ino4p form a complex, and bind to UAS_{INO} sequence and activate the transcription of *INO1* and other phospholipid biosynthetic genes (Henry et al. 2012). Both the *ino2*Δ and *ino4*Δ cells exhibit inositol auxotrophy, and down regulate the *INO1* expression (Henry et al. 2012; Bachhawat et al. 1995; Shetty and Lopes 2010). In *gcr1*Δ cells, the mRNA expression of *INO2* was significantly down regulated (in both I− and I+ condition) accounting for the reduction in inositol and *INO1* transcription (Fig. 2e).

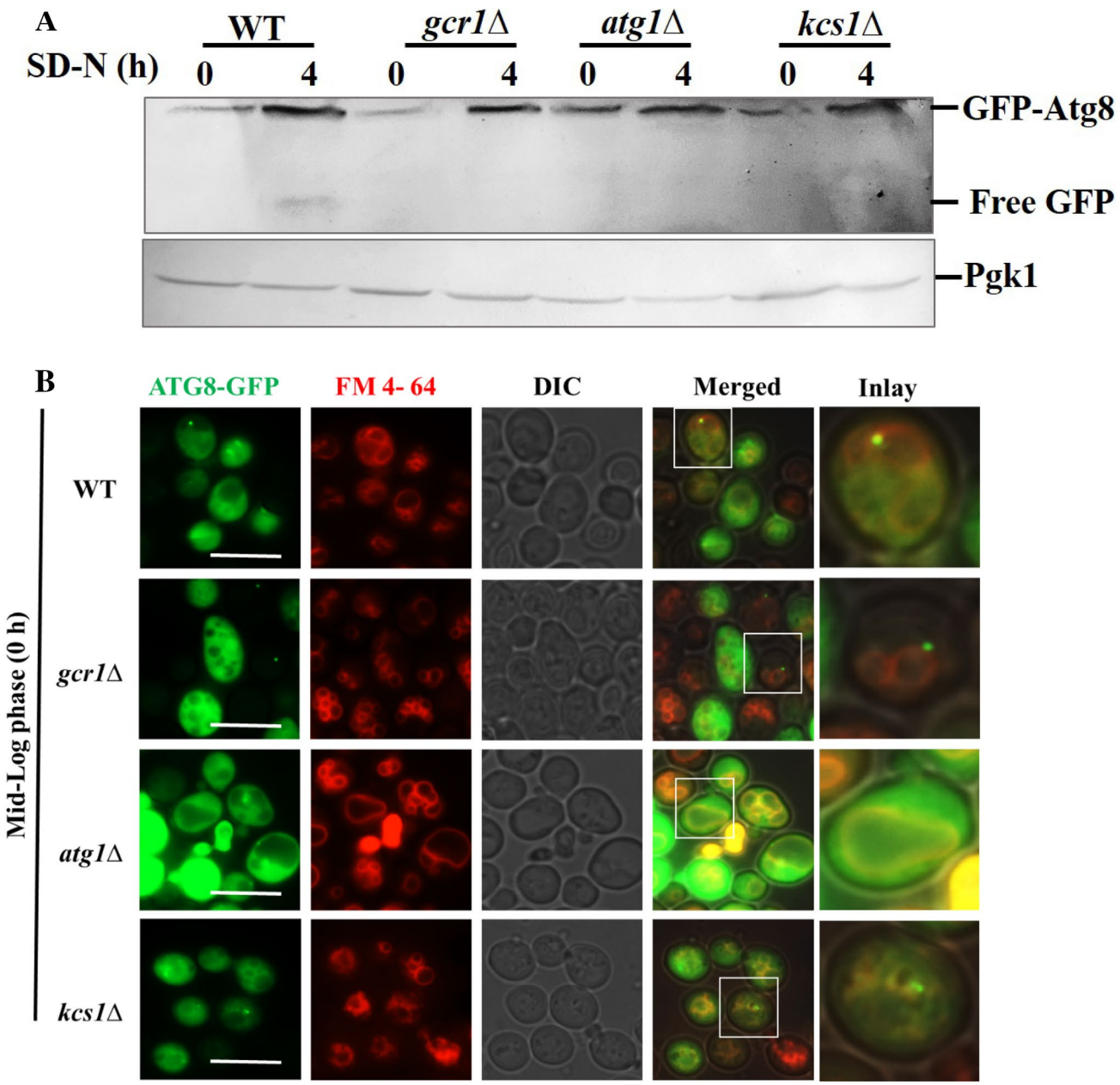

Fig. 9 *GCR1* deletion affects autophagy process analyzed by western blotting and fluorescent microscopy. The WT and deletion strains (*gcr1*Δ, *atg1*Δ, and *kcs1*Δ) were transformed with the pRS315-Atg8–GFP expression plasmid. The transformants were grown up to mid-log phase in SD-Ura (0 h), followed by induction with nitrogen starvation media (SD-N) for 4 h. **a** GFP–Atg8 cleavage by immunoblotting analysis. Samples were collected and the cleavage of Atg8–GFP was analyzed by immunoblotting with anti-GFP antibody that detected both Atg8–GFP (40 kDa) and free GFP (26 kDa). The Pgk1 (45 kDa) served as loading control. **b** and **c** Fluorescent microscopic analysis of Atg8–GFP localization and FM 4–64 dye (vacuolar morphology) in WT, *gcr1*Δ, *kcs1*Δ, and *atg1*Δ cells. The cells were collected and the images were captured using Axio Observed 3 Inverted fluorescence microscope (Zeiss) with an excitation wavelength of 488 nm for Green fluorescence and 514 nm for FM 4–64. Scale bar, 5 µm. **d** Ape1 processing assay by immunoblotting. The WT, *gcr1*Δ, *atg1*Δ and *kcs1*Δ cells were grown up to mid-log phase in SC media and starved for 4 h in SD-N media. The cells were collected, and protein extracted and analyzed by immunoblotting with Ape1 antibody (prApe1 ~ 60 kDa; mApe1 ~ 50 kDa size; Asterisk denotes non-specific band). The data are represented as three independent repeats. prApe1, precursor Ape1; mApe1, mature Ape1

The *PIS1* gene contains a predicted consensus sequence (CTTCC) for the transcription factor *GCR1* (Gardocki and Lopes 2003). The expression of *PIS1* was down regulated in *gcr1*Δ strain, resulting in decreased cellular PI level compared to WT (Fig. 3a, b). The *PIS1-LacZ* was measured by β-galactosidase activity and a reduction was observed in *gcr1*Δ cells both in the presence and absence of inositol (Fig. 3c). The PI level was reduced under

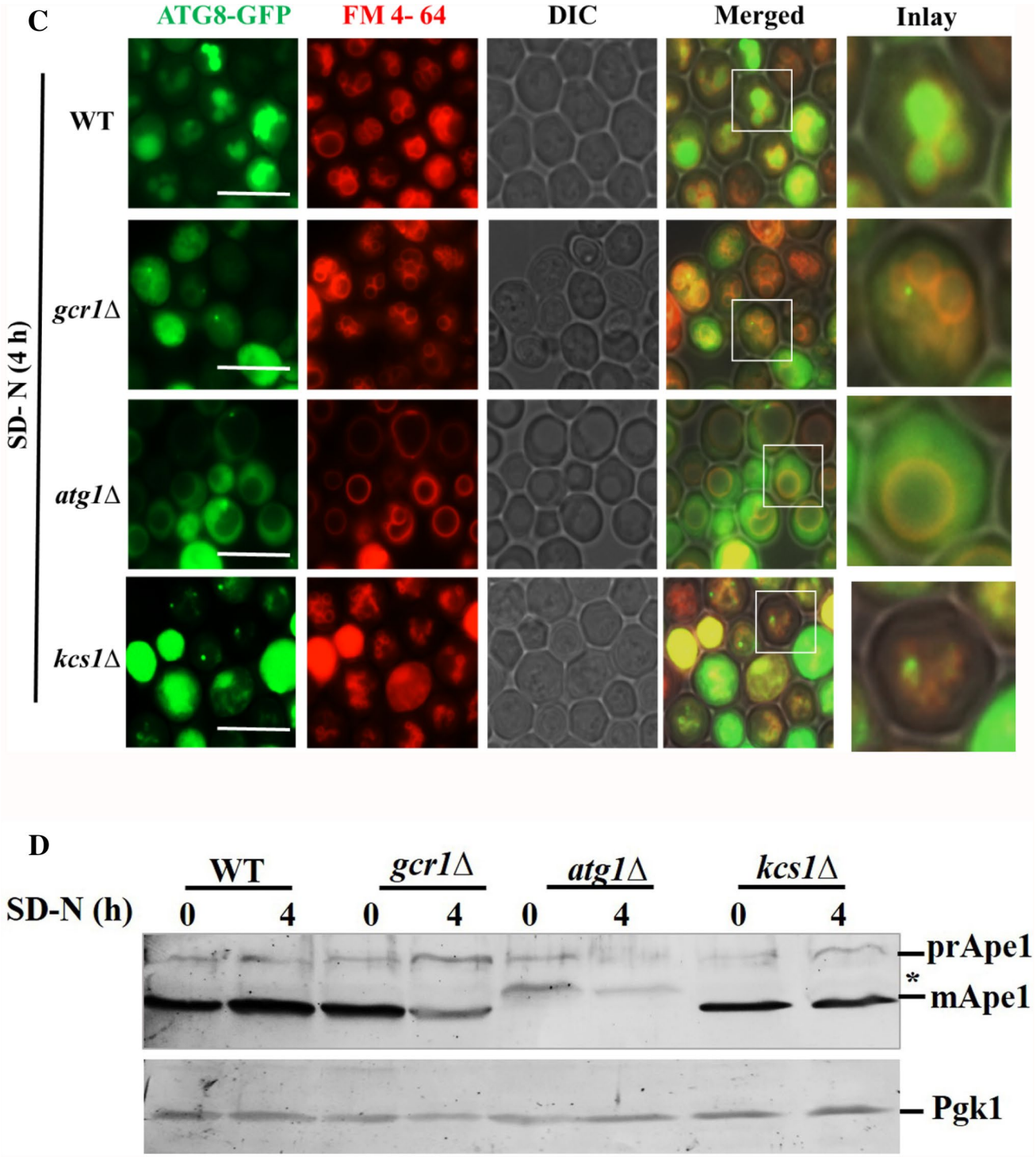

Fig. 9 (continued)

inositol deprivation compared to the inositol presence in WT cells (Fig. 3a), which altered the lipid derivatives including sphingolipid, phosphoinositides (Jesch et al. 2010; Henry et al. 2014), and GPI anchor (Doering and Schekman 1996).

We found a reduced expression of Gcr1 under I− in WT cells (Fig. 4) and this could be attributed to the increased expression of Kcs1p (Fig. 5c) and phosphoinositides metabolism under I− (Jesch et al. 2010; Ye et al. 2013; Henry et al. 2014). The exogenous inositol supplementation increased

glycolytic pathway and generated more ATP (Deranieh et al. 2015), and also increased Gcr1p expression in WT-pRS315-*GCR1* cells (Fig. 4). The Kcs1p produces 5PP-IP4 that binds with Ino2p–Ino4p complex and activates the *INO1* expression (Ye et al. 2013). On the other hand, Kcs1p forms pyrophosphate 5PP-IP5 which binds to Gcr1p and reduces its binding with Gcr2p that affected G*CR1* mediated transcriptional regulation (Szijgyarto et al. 2011). The expression of Kcs1p was increased under inositol limitation condition (Fig. 5c), and is important for optimal *INO1* transcription and inositol production in yeast (Ye et al. 2013). The Kcs1p expression in *gcr1*Δ cells, was reduced in both I− and I+ condition compared to WT I− (Fig. 5c) validating the reduced *INO1* transcription and inositol growth defect in *gcr1*Δ strain. The *INO1* transcription was initiated by epigenetic transcriptional memory under inositol deprivation, through Sfl1p transcription factor (D'Urso and Brickner 2017). The Gcr1p regulates RNA polymerase II transcription (Santangelo 2006; Menon et al. 2005), and its mutation reduced *INO1* transcription (Berroteran et al. 1994; Henry et al. 2014). Aforementioned, the loss of Gcr1p exhibited inositol dependent growth defect and it might be due to the misregulation of *INO1* transcription (Ye et al. 2013) and the expression of *GCR1*in the *gcr1*Δ strain rescued the growth defect and *INO1* expression under inositol deprivation (Fig. 7). The over expression of *GCR1* in WT cells, did not change the level of *INO1* expression and this could be due to the influence of Kcs1p under inositol deprivation (Fig. 7).

The defect in *KCS1* depicted a defect in vacuolar membrane morphology (Saiardi et al. 2002; Dubois et al. 2002). The deletion of Ino1p exhibited vacuolar membrane dynamics and affects endocytosis under inositol limitation (Deranieh et al. 2015). The defective vacuolar morphology was increased in *gcr1*Δ cells, and *kcs1*Δ cells and both depicted a similar phenotype (Fig. 8). The *gcr1*Δ cells decreased the Kcs1p expression and thereby accounted for the defective vacuolar membrane. The *gcr1*Δ cells reduced vacuolar Atg8–GFP co-localization under nitrogen starvation compared to WT cells (Fig. 7c). There is an accumulation of Atg8–GFP punctuate in the cytosol in *gcr1*Δ cells under SD-N (4 h and 8 h) (Fig. S4). Kcs1p is required for proper localization of PAS for autophagosomal formation under nitrogen starvation (Taylor et al. 2012). The formation of mApe1 is reduced under nitrogen starvation in the *gcr1*Δ cells (Fig. 9d). Previous, study suggested that *gcr1*Δ strain is not affected by rapamycin (Menon et al. 2005; Lieb et al. 2001).

In summary, based on our findings we suggest that Gcr1p positively controls *PIS1* transcription, and the deletion of *GCR1* affects the Kcs1p which declines *INO1* expression that resulted in inositol-dependent growth defect, vacuolar abnormality and autophagy defect in yeast. The potential regulatory role of Gcr1p in lipid metabolism is still elusive and yet to be explored.

Acknowledgements This work was supported by the Science and Engineering Research Board (SERB) Grant No: EMR/2016/001727, New Delhi, under EMR scheme. C. Ravi was supported by a fellowship from SERB, New Delhi. We are grateful to Prof. Ram Rajasekharan (Central Food Technological Research Institute, Mysore, India) for providing yeast strains, over expression plasmids, reagents and instrument facility. We thank Prof. Rashna Bhandari (Centre for DNA Fingerprinting and Diagnostics, India), and John M. Lopes (College of Natural Sciences, University of Massachusetts, Amherst, MA) for providing pYES2-*KCS1* and YEp357R-*INO1*-LacZ plasmids. We thank Prof. Tracy L. Johnson (Molecular Cell and Developmental Biology, University of California, Los Angeles, CA 90095, USA), Prof. Ji-Sook Hahn (School of Chemical and Biological Engineering, Seoul National University, Seoul, Korea), and Prof. Ravi Manjithaya (Molecular Biology and Genetics Unit, Jawaharlal Nehru Centre for Advanced Scientific Research Jakkur, Bangalore 560 064, India) for providing plasmids pRS315-*GCR1*-TAP tag, pRS415GPD, pRS415GPD-*GCR1* and pRS316–ATG8–GFP, respectively. We thank Prof, Yoshinori Oshsumi (Tokyo Institute of Technology, Yokohama, Japan) for providing Ape1 antiserum. We are thankful for the infrastructure facilities of DST-FIST, Department of Biochemistry, Life Sciences and DST-PURSE facilities, of Bharathidasan University.

Author contributions V.N. and C.R designed the experiments. C.R and R.G performed the experiments. C.R and V.N. discussed the data and wrote the paper. All authors reviewed the results and approved the final version of the manuscript.

References

Abramoff MD, Magelhaes PJ, Ram SJ (2004) Image processing with Image J. Biophoton Int 11:36–42

Anderson MS, Lopes JM (1996) Carbon source regulation of PIS1 gene expression in *Saccharomyces cerevisiae* involves the MCM1 gene and the two-component regulatory gene, SLN1. J Biol Chem 271:26596–26601

Bachhawat N, Ouyang Q, Henry SA (1995) Functional characterization of an inositol-sensitive upstream activation sequence in yeast. A cis-regulatory element responsible for inositol choline-mediated regulation of phospholipid biosynthesis. J Biol Chem 270:25087–25095

Baker HV (1986) Glycolytic gene expression in saccharomyces cerevisiae: nucleotide sequence of *GCRI*, null mutants, and evidence for expression. Mol Cell Biol 11:3774–3784

Baker HV (1991) GCR1 of *Saccharomyces cerevisiae* encodes a DNA binding protein whose binding is abolished by mutations in the CTTCC sequence motif. Proc Natl Acad Sci USA 88:9443–9447

Barbara KE, Haley TM, Willis KW, Santangelo GM (2006) The transcription factor Gcr1 stimulates cell growth by participating in nutrient-responsive gene expression on a global level. Mol Genet Genom 277:171–188

Becker GW, Lester RL (1977) Changes in phospholipids of *Saccharomyces cerevisiae* associated with inositol-less death. J Biol Chem 252:8684–8691

Berroteran RW, Ware DE, Hampsey M (1994) The sua8 suppressors of *Saccharomyces cerevisiae* encode replacements of conserved residues within the largest subunit of RNA polymerase II and affect transcription start site selection similarly to sua7 (TFIIB) mutations. Mol Cell Biol 14:226–237

Bligh EG, Dyer WJ (1959) A rapid method of total lipid extraction and purification. Can J Biochem Physiol 37:911–917

Bradford MM (1976) A rapid and sensitive method for the quantitation of microgram quantities of protein utilizing the principle of protein-dye binding. Anal Biochem 72:248–254

Bryant NJ, Stevens TH (1998) Vacuole biogenesis in *Saccharomyces cerevisiae*: Protein transport pathways to the yeast vacuole. Microbiol Mol Biol Rev 62:230–247

Carman GM, Han GS (2007) Regulation of phospholipid synthesis in *Saccharomyces cerevisiae* by zinc depletion. Biochim Biophys Acta 1771:322–330

Carman GM, Han GS (2011) Regulation of phospholipid synthesis in the yeast *Saccharomyces cerevisiae*. Annu Rev Biochem 80:859–883

Chirala SS (1992) Coordinated regulation and inositol-mediated and fatty acid-mediated repression of fatty acid synthase genes in *Saccharomyces cerevisiae*. Proc Natl Acad Sci USA 89:10232–10236

Clifton D, Fraenkel DG (1981) The gcr (glycolysis regulation) mutation of *Saccharomyces cerevisiae*. J Biol Chem 256:13074–13078

D'Urso A, Brickner JH (2017) Epigenetic transcriptional memory. Curr Genet 63:435–439

Deranieh RM, Shi Y, Tarsio M, Chen Y, McCaffery JM, Kane PM, Greenberg ML (2015) Perturbation of the vacuolar ATPase A Novel Consequence Of Inositol Depletion. J Biol Chem 290:27460–27472

Doering TL, Schekman R (1996) GPI anchor attachment is required for Gas1p transport from the endoplasmic reticulum in COP II vesicles. EMBO J 15:182–191

Donahue TF, Henry SA (1981) myo-Inositol-1-phosphate synthase. Characteristics of the enzyme and identification of its structural gene in yeast. J Biol Chem 256:7077–7085

Dubois E, Scherens B, Vierendeels F, Ho MM, Messenguy F, Shears SB (2002) In *Saccharomyces cerevisiae*, the inositol polyphosphate kinase activity of Kcs1p is required for resistance to salt stress, cell wall integrity, and vacuolar morphogenesis. J Biol Chem 277:23755–23763

Gardocki ME, Lopes JM (2003) Expression of the yeast *PIS1* Gene requires multiple regulatory elements including a Rox1p binding site. J Biol Chem 278:38646–38652

Gardocki ME, Bakewell M, Kamath D, Robinson K, Borovicka K, Lopes JM (2005) Genomic Analysis of PIS1 Gene Expression. Eukaryotic cell 4:604–614

Gaspar ML, Aregullin MA, Jesch SA, Henry SA (2006) Inositol induces a profound alteration in the pattern and rate of synthesis and turnover of membrane lipids in *Saccharomyces cerevisiae*. J Biol Chem 281:22773–22785

Gaspar ML, Hofbauer HF, Kohlwein SD, Henry SA (2011) Coordination of storage lipid synthesis and membrane biogenesis: evidence for cross-talk between triacylglycerol metabolism and phosphatidylinositol synthesis. J Biol Chem 286:1696–1708

Gietz RD, Schiestl RH (2007) High-efficiency yeast transformation using the LiAc/SS carrier DNA/PEG method. Nat Protoc 2:31–34

Greenberg ML, Reiner B, Henry SA (1982) Regulatory mutations of inositol biosynthesis in yeast: isolation of inositol-excreting mutants. Genetics 100:19–33

Han SH, Han GS, Iwanyshyn WM, Carman GM (2005) Regulation of the PIS1-encoded phosphatidylinositol synthase in *Saccharomyces cerevisiae* by zinc. J Biol Chem 280:29017–29024

Hellman LM, Fried MG (2007) Electrophoretic mobility shift assay (EMSA) for detecting protein-nucleic acid interactions. Nat Protoc 2:1849–1861

Henry SA, Kohlwein SD, Carman GM (2012) Metabolism and regulation of glycerolipids in the yeast *Saccharomyces cerevisiae*. Genetics 190:317–349

Henry SA, Gaspar ML, Jesch SA (2014) The response to inositol: Regulation of glycerolipid metabolism and stress response signaling in yeast. Chem Phys Lipids 180:23–43

Hossain MA, Claggett JM, Edwards SR1, Shi A, Pennebaker SL, Cheng MY, Hasty J, Johnson TL (2016) Posttranscriptional Regulation of Gcr1 Expression and Activity Is Crucial for Metabolic Adjustment in Response to Glucose Availability. Mol Cell 62:346–358

Huie MA, Scott EW, Drazinic CM, Lopez MC, Hornstra IK, Yang TP, Baker HV (1992) Characterization of the DNA-Binding Activity of GCR1: In Vivo Evidence for Two GCR1-Binding Sites in the Upstream Activating Sequence of TPI of *Saccharomyces cerevisiae*. Mol Cell Biol 6:2690–2700

Jackson JC, Lopes JM (1996) The yeast UME6 gene is required for both negative and positive transcriptional regulation of phospholipid biosynthetic gene expression. Nucleic Acids Res 24:1322–1329

Jesch SA, Gaspar ML, Stefan CJ, Aregullin MA, Henry SA (2010) Interruption of inositol sphingolipid synthesis triggers Stt4p-dependent protein kinaseC signaling. J Biol Chem 285:41947–41960

Kamada Y, Yoshino K, Kondo C, Kawamata T, Oshiro N, Yonezawa K, Ohsumi Y (2010) Tor directly controls the Atg1 kinase complex to regulate autophagy. Mol Cell Biol 30:1049–1058

Kliewe F, Kumme J, Grigat M, Hintze S, Schüller HJ (2017) Opi1 mediates repression of phospholipid biosynthesis by phosphate limitation in the yeast *Saccharomyces cerevisiae*. Yeast 34:67–81

Lenburg ME, O'Shea EK (2001) Genetic evidence for a morphogenetic function of the *Saccharomyces cerevisiae* Pho85 cyclin dependent kinase. Genetics 157:39–51

Li SC, Kane PM (2009) The yeast lysosome-like vacuole: endpoint and crossroads. Biochim Biophys Acta 1793:650–663

Lieb JD, Liu X, Botstein D, Brown PO (2001) Promoter-specific binding of Rap1 revealed by genome-wide maps of protein-DNA association. Nat Genet 28:327–334

Livak KJ, Schmittgen TD (2001) Analysis of relative gene expression data using real-time quantitative PCR and the 2(–Delta Delta C (T)) method. Methods 25:402–408

Loewen CJ, Gaspar ML, Jesch SA, Delon C, Ktistakis NT, Henry SA, Levine TP (2004) Phospholipid metabolism regulated by a transcription factor sensing phosphatidic acid. Science 304:1644–1647

Menon BB, Sarma NJ, Pasula S, Deminoff SJ, Willis KA, Barbara KE, Andrews B, Santangelo GM (2005) Reverse recruitment: the Nup84 nuclear pore subcomplex mediates Rap1/Gcr1/Gcr2 transcriptional activation. Proc Natl Acad Sci USA 102:5749–5754

Murray M, Greenberg ML (2000) Expression of yeast INM1 encoding inositol monophosphatase is regulated by inositol, carbon source, and growth stage and is decreased by lithium and valproate. Mol Microbiol 36:651–661

Nikawa J, Kodaki T, Yamashita S (1987) Primary structure and disruption of the phosphatidylinositol synthase gene of Saccharomyces cerevisiae. J Biol Chem 262:4876–4881

Rajvanshi PK, Arya M, Rajasekharan R (2017) The stress-regulatory transcription factors Msn2 and Msn4 regulate fatty acid oxidation in budding yeast. J Biol Chem 292:18628–18643

Rao MJ, Srinivasan M, Rajasekharan R (2017) Cell size is regulated by phospholipids and not by storage lipids in *Saccharomyces cerevisiae*. Curr Genet 64:1071–1087

Rose M, Botstein D (1983) Construction and use of gene fusions to lacZ (β- galactosidase) that are expressed in yeast. Methods Enzymol 101:167–180

Rouser G, Siakotos AN, Fleischer S (1966) Quantitative analysis of phospholipids by thin layer chromatography and phosphorus analysis of spots. Lipids 1:85–86

Saiardi A, Sciambi C, McCaffery JM, Wendland B, Snyder SH (2002) Inositol pyrophosphates regulate endocytic trafficking. Proc Natl Acad Sci 99:14206–14211

Saiardi A, Resnick AC, Snowman AM, Wendland B, Snyder SH (2005) Inositol pyrophosphates regulate cell death and telomere length through phosphoinositide 3-kinase-related protein kinases. Proc Natl Acad Sci 102:1911–1914

Sambrook J, Fritsch EF, Maniatis T (1989) Molecular cloning, a laboratory manual, 2nd edn. Cold Spring Harbor Laboratory, Cold Spring Harbor, pp 6.55–6.56

Santangelo GM (2006) Glucose signaling in *Saccharomyces cerevisiae*. Microbiol Mol Biol Rev MMBR 70:253–282

Seker T, Hamamci H (2003) Trehalose, Glycogen and Ethanol metabolism in the *gcr1* Mutant of *Saccharomyces cerevisiae*. Folia Microbiol (Praha) 48:193–198

Shetty A, Lopes JM (2010) Derepression of INO1 transcription requires cooperation between the Ino2p-Ino4p heterodimer and Cbf1p and recruitment of the ISW2 chromatin-remodeling complex. Eukaryot cell 12:1845–1855

Shi Y, Vaden DL, Ju S, Ding D, Geiger JH, Greenberg ML (2005) Genetic perturbation of glycolysis results in inhibition of *de novo* inositol biosynthesis. J Biol Chem 280:41805–41810

Shintani T, Klionsky DJ (2004) Cargo proteins facilitate the formation of transport vesicles in the cytoplasm to vacuole targeting pathway. J Biol Chem 279:29889–29894

Stauffer B, Powers T (2017) Target of rapamycin signaling mediates vacuolar fragmentation. Curr Genet 63:35–42

Sugimoto K (2018) Branching the Tel2 pathway for exact fit on phosphatidylinositol 3-kinase-related kinases. Curr Genet 64:965–970

Suzuki K, Ohsumi Y (2007) Molecular machinery of autophagosome formation in yeast, *Saccharomyces cerevisiae*. FEBS Lett 581:2156–2161

Szijgyarto Z, Garedew A, Azevedo C, Saiardi A (2011) Influence of inositol pyrophosphates on cellular energy dynamics. Science 334:802–805

Taylor R Jr, Chen PH, Chou CC, Patel J, Jin SV (2012) *KCS1* deletion in *Saccharomyces cerevisiae* leads to a defect in translocation of autophagic proteins and reduces autophagosome formation. Autophagy 8:1300–1311

Tornow J, Zeng X, Gao W, Santangelo GM (1993) *GCR1*, a transcriptional activator in *Saccharomyces cerevisiae*, complexes with *RAP1* and can function without its DNA binding domain. EMBO J 12:2431–2437

Turkel S, Turgut T, Lopez MC, Uemura H, Baker HV (2003) Mutations in GCR1 affect SUC2 gene expression in *Saccharomyces cerevisiae*. Mol Gen Genom 268:825–831

Vida TA, Emr SD (1995) A new vital stain for visualizing vacuolar membrane dynamics and endocytosis in yeast. J Cell Biol 128:779–792

Wang CW, Klionsky DJ (2003) The molecular mechanism of autophagy. Mol Med 9:65–76

Willis KA, Barbara KE, Menon BB, MoVat J, Andrews B, Santangelo GM (2003) The global transcriptional activator of *Saccharomyces cerevisiae*, Gcr1p, mediates the response to glucose by stimulating protein synthesis and *CLN*-dependent cell cycle progression. Genetics 165:1017–1029

Ye C, Bandara WM, Greenberg ML (2013) Regulation of Inositol metabolism is fine-tuned by inositol pyrophosphates in *Saccharomyces cerevisiae*. J Biol Chem 288:24898–24908

York JD, Guo S, Odom AR, Spiegelberg BD, Stolz LE (2001) An expanded view of inositol signaling. Adv Enzyme Regul 41:57–71